Chapter 7
Optical Diagnostics for Gasoline Direct Injection Engines

Ankur Kalwar and Avinash Kumar Agarwal

Abstract Advancements in internal combustion (IC) engine technologies have improved both spark ignition (SI) and compression ignition (CI) engines immensely in terms of fuel efficiency and emissions. Gasoline engines are giving tough competition to their diesel counterparts in the light-duty passenger car segment with continuously increasing market share. Apart from lower exhaust emissions, current generation Gasoline Direct Injection (GDI) engines offer higher power output and superior fuel economy. Nevertheless, automotive researchers and engineers have used many tools to evolve state-of-the-art GDI engine technology continuously. The most important and useful tool in engine development is optical diagnostics. Optical access to the engine allows non-intrusive investigations of the in-cylinder processes using optical/laser-based diagnostics, which provides information not available by any other research tool. This chapter discusses applying such techniques to understand various in-cylinder processes such as spray-flow interactions, fuel–air mixture formation, combustion, and pollutant formation in GDI engines. It includes detailed perspectives that help optimize engine design and control parameters adapted to conventional and alternative fuels. It broadly covers studies related to in-cylinder flow characteristics, sprays characterization, fuel spray-air interactions, fuel evaporation, mixture formation, flame propagation characteristics, and pollutant formation, corresponding to different GDI engine operating parameters. This chapter discusses applications of various optical diagnostic techniques in GDI engine investigations such as particle imaging velocimetry (PIV), Mie-scattering, phase Doppler interferometry (PDI), laser-induced fluorescence (LIF), natural flame chemiluminescence, laser-induced incandescence (LII), OH/CH chemiluminescence. The rich information derived from the optical diagnostic techniques helps develop new-generation GDI engines capable of meeting market requirements and emission compliance.

Keywords Gasoline direct injection · Optical diagnostics · In-cylinder flows · Spray · Charge distribution · Pollutant formation

A. Kalwar · A. K. Agarwal (✉)
Engine Research Laboratory, Department of Mechanical Engineering, Indian Institute of Technology Kanpur, Kanpur 208016, India
e-mail: akag@iitk.ac.in

A. K. Agarwal et al. (eds.), *Advanced Combustion for Sustainable Transport*, Energy, Environment, and Sustainability, https://doi.org/10.1007/978-981-16-8418-0_7

7.1 Introduction

This section introduces the state of development in Gasoline direct injection (GDI) engines. Limitations of current GDI engines are also discussed. After this, the need and role of optical diagnostics in GDI engine development are also explained. Since the invention of IC engines, unthrottled engine operation, and efficient control are considered promising. This helps avoid pumping losses and improves combustion efficiency. Thermodynamics conditions suitable for efficient combustion are always attained in such conditions. Heat is released in a mixing-controlled combustion process by auto-ignition of diesel vapours wherever they are in a combustion chamber. In gasoline engines, unthrottled engine operation and predominantly mixing-controlled combustion are difficult due to homogeneous mixture formation and constraints of fixed location of the spark plug. This imposes additional restrictions on the mixture formation process in SI engines. In addition to temporal fuel evaporation requirement, the spatial evolution of repeatable fuel–air mixture distribution is required for a stable stratified mixture formation in every engine cycle. However, homogeneous combustion in the GDI engine does not face any such difficulty related to the charge preparation. With the evolution of the GDI engine technology over time, many measures have been taken to ensure that the combustion system fulfils these requirements (Fraidl et al. 1996). The stratification of the fuel–air mixture is achieved by injecting the fuel into a sub-volume of the combustion chamber, creating well-separated zones with rich, stoichiometric, and lean fuel–air mixtures. This stratified charge combustion engine can be operated with an overall leaner fuel–air mixture, enhancing the fuel economy. The main combustion systems investigated for achieving stratified charge combustion could be air-guided, wall-guided, and spray-guided configurations. Among these, the latter two are the most commonly used, in which spray-guided configuration is considered a new generation GDI engine. Nevertheless, these combustion systems face the problems of wall impingement of sprays, higher HC and soot emissions, limited range of engine operation, and non-repeatability of charge formation. Successful combustion of stratified mixture with lower emissions requires controlled in-cylinder airflow, precise fuel injection, enhanced fuel spray evaporation, optimum fuel–air mixture distribution, and accurate charge motion. Maintaining all these parameters in an optimum range is a challenging task. Several studies have optimized control parameters such as controlled intake flow, combustion chamber design, injector parameters, and fuel injection strategies to achieve desirable engine performance. Our previous chapter describes a detailed analysis of these studies (Kalwar and Agarwal 2020).

Developing sophisticated and new tools for 3D CFD simulations and optical diagnostics has helped obtain newer insights into an engine's complex mixture formation and combustion processes. The availability of these tools helps in further refinement of the overall combustion system of GDI engines. The future development targets for new GDI engines include reducing fuel consumption, improving the engine performance with minimum compromise on fuel economy, and meeting the existing and upcoming emission norms. For emission legislation compliance,

exhaust after-treatment technologies such as TWC, particulate trap, DeNOx, etc., are also incorporated in GDI engines. It is expected that cost of GDI vehicles should be comparable with current MPFI vehicles. It is also essential to optimize various parameters for cold-start, transient, and warm-engine conditions and switch between different operating modes of the GDI engine.

In the last couple of decades, the application and functionalities of optical diagnostics of engines have seen dramatic growth in engine research and development. Their crucial role in developing better engines has led to their transition from esoteric research tools to mainstream development tools. Direct observation of flame kernel initiation, flame growth, propagation, and extinction and its correlation with in-cylinder pressure data have rapidly gained importance. The developments in lasers and digital cameras have given a big boost to optical diagnostic tools. It enabled the measurements of various intrinsic processes such as highly spatially and temporally resolved fuel vaporization and multi-dimensional distribution of temperature, flow-fields, and pollutant concentration. These capabilities are of vital importance in modern engine development (Sick 2010). Optimized multi-phase flows, spray-wall impingement, stratification of charge, premixed charge combustion, formation of soot and other pollutants, and other phenomena of importance in carburettor/port injection have become crucial for the success of GDI engines. The cycle-to-cycle variability has become an important aspect of these investigations. The combustion modes involving lean and stratified mixtures result in a high likeliness that the mixtures exceed the flammability limit, eventually leading to misfire (Kalwar and Agarwal 2021). This chapter reviews and summarizes the application of various optical diagnostic techniques to study such aspects for different engine control parameters.

Exploring fundamental physical and chemical processes that control engine operation is essential for improving IC engines. However, it is impossible to evaluate a large number of engine concepts and operation conditions. In addition to being time-consuming and cost-intensive processes, this approach also risks missing the overall optimum. Hence, one of the important areas for optical diagnostics is to aid, develop and calibrate CFD simulation tools for IC engines. Fully predictive numerical models for engine-related processes are gaining significance. Although, considerable differences in the thermal properties of the optical engine with its metal engine counterpart lead to difficulties in matching their combustion characteristics. However, fundamental physics is not much affected by this. These limitations could be avoided by directly applying optical diagnostics on realistic and production-grade engine geometries. This requires greater emphasis on developing micro and small-sized sensors/diagnostics that only need small optical access, e.g., fibre optics could be used for data collection and illumination in some of these techniques.

7.2 Optical Diagnostics in GDI Engines

Over the last couple of decades, several optical diagnostic tools have been developed, applied, and used for GDI engine investigations (Sick 2010). Direct injection of fuel, the multi-phase nature of the in-cylinder charge, and spray-wall interactions pose challenges in implementing optical diagnostic techniques in the engines. This section presents a detailed discussion of all such important phenomena investigated using various optical diagnostic tools. Effect of different engine control parameters, operating conditions, and fuel types are analyzed for the in-cylinder spray characterization, in-cylinder flows, spray-flow interactions, charge formation, flame characterization, and pollutant formation.

7.2.1 In-cylinder Spray Characterization

In-cylinder investigations of spray characteristics provide realistic insights into the fuel injection process and spray quality. Many researchers have successfully attempted high-speed imaging of fuel spray in an optical GDI engine (Catapano et al. 2013; Lee et al. 2020). Mie scattering technique is widely used for visualizing the in-cylinder injection process and characterizing GDI spray.

In a study by Catapano et al. (2013), in-cylinder spray imaging was done by an Intensified Charge-Coupled Device (ICCD) camera with sensitivity in 200–800 nm wavelength covering both UV and visible spectrum in the wall-guided GDI engine. Images were recorded via the piston optical window, and CW halogen lamps were used for illuminating the flow through the optical liner, as shown in Fig. 7.1. The acquired images were post-processed using Labview software and National Instruments hardware. The procedure for obtaining results from the raw spray images is shown in Fig. 7.2. Initially, a raw 12-bit colour image was converted to a 12-bit greyscale image. After this, the image underwent convolution filtering and was binarized by applying a 15% threshold for instantaneous luminosity. Finally, the outline was created by selecting the region of interest. Spray penetration was measured by assessing the maximum distance between the fuel injector and the spray tip.

Fuel injection parameters were the most critical factors affecting the spray characteristics. A substantial number of studies have investigated the impact of fuel injection parameters such as fuel injection timing, fuel injection pressure (FIP), and injection strategies on the in-cylinder spray characteristics. In a study by Lee et al. (2020), the effects of fuel injection timing and FIP on the spray behaviour and wall impingement in a DISI optical engine having a wall-guided configuration were studied. The spray images obtained at 8° CA after the fuel injection were considered for assessing the spray development. The spray collapsed when it reached the optically accessible window, and there were hardly any differences to distinguish the plumes. For injection timing at 330° bTDC or before, spray directly impacted the piston even before

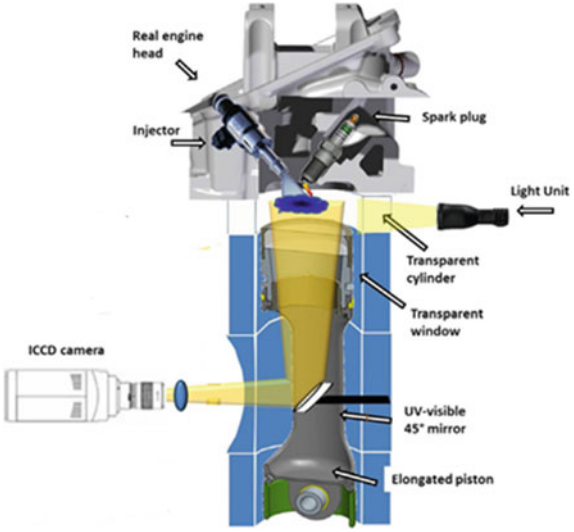

Fig. 7.1 Schematic of the experimental setup of optical GDI engine for digital imaging (Catapano et al. 2013)

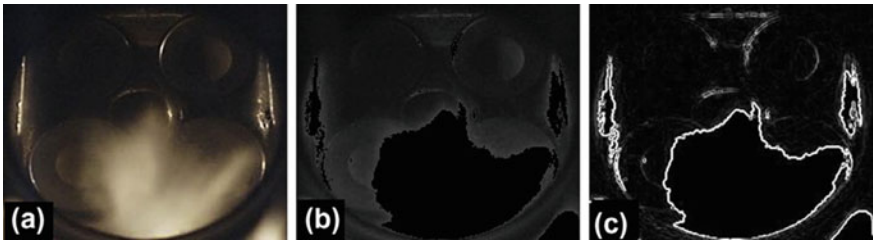

Fig. 7.2 Steps for post-processing of data for calculating the spray penetration (Catapano et al. 2013)

getting completely atomized and evaporated. Due to the shorter distance for injection, in-cylinder flow was quite weak in such a case, and spray behaviour was mainly dependent on the spray momentum. For 300° bTDC injection timing, the spray shape demonstrated bowed trajectory, mainly due to in-cylinder flow in reverse direction w.r.t. the injection during the intake process. This led to the bending of spray towards the injector, causing wetting of the cylinder walls. The spray travelled straight for the injection timing of 270° bTDC or later. These characteristics were in agreement with the variations in the in-cylinder flow during the intake process. At a late injection timing of 210° bTDC, the in-cylinder flow intensity reduced as the maximum valve lift was completed. Hence, injected fuel spray hardly faced any noticeable disruption and travelled straight. Towards the end of injection, the spray tip reached the cylinder wall on the opposite side of the injector, resulting in wall-film formation.

The spray development was further investigated for variations in the FIP at 300° and 210° bTDC injection timing, as shown in Fig. 7.3. The spray penetration was higher for late injection timing than the advanced one, with an increasing FIP. The spray was minimally affected by the ambient flow and was mainly driven by its momentum. Hence, a larger straight movement of the spray led to greater fuel mass reaching the cylinder walls. For fuel injection at 300° bTDC, increasing the FIP enhanced the horizontal movement of spray in the rightward direction. The higher FIP improved the atomization of spray droplets. Hence smaller droplets suffered greater deflection due to in-cylinder flows. The elevated rightward deflection of spray encountered the spray penetration and increased the wall-wetting on the injector side on the cylinder wall. However, spray deviation diminished and inhibited penetration at higher load due to higher ambient gas pressure.

Moreover, spray deviation images were obtained from 50 consecutive injection cycles. The regions of high variations in spray evolution were located for both early and late injection timings. For 300° bTDC, large variations were observed in the lower-right section of the spray, where the spray bending occurred. This region was mainly influenced by turbulence and strong in-cylinder flow movement, which augmented variations in the spray behaviour. These variations were reinforced at higher FIP. For late injection timing of 210° bTDC, the lower part of the spray underwent larger variations. This was mainly because of the turbulence created by the air entrainment in the spray. The low-pressure zone formed on the lower side of

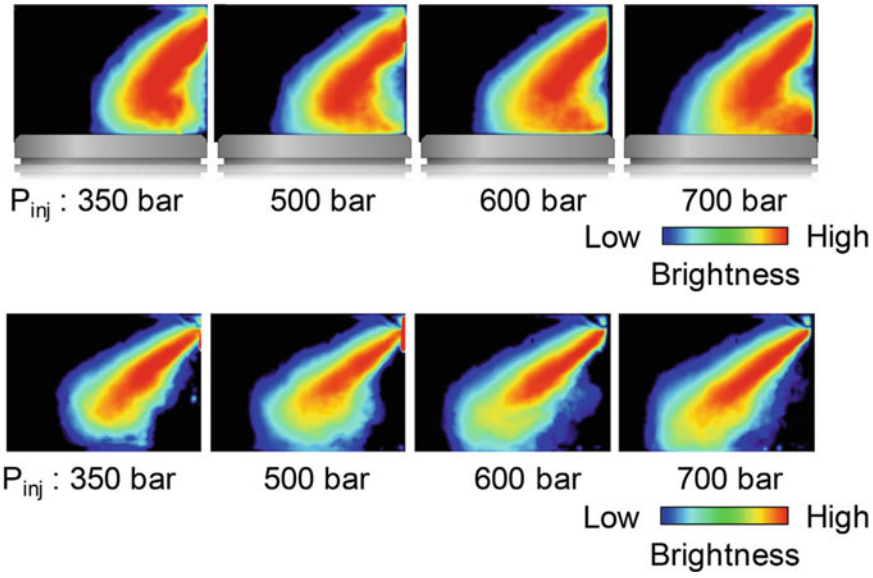

Fig. 7.3 In-cylinder spray behaviour at 300° bTDC and 210° bTDC injection timing with an increased pressure (Lee et al. 2020)

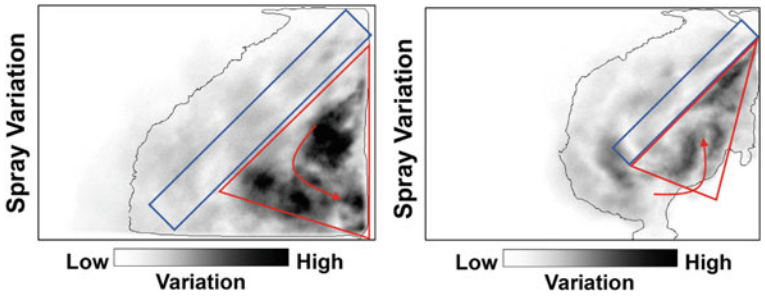

Fig. 7.4 Spray variations for injection timing of 300° bTDC (600 bar pressure) and 210° bTDC (350 bar pressure) (Lee et al. 2020)

the spray by the drag of ambient air due to high-speed droplets resulted in an inflow of air stream. Hence, this region faced larger variations, as shown in Fig. 7.4.

Findings by Song and Park (2015) reported that spray development differed in the engine than the quiescent chamber due to the piston motion. Injecting fuel at 180° aTDC (end of intake stroke) resulted in similar spray morphology to the chamber. Despite turbulence in the engine cylinder, weak intake flow due to the absence of piston motion at BDC didn't affect the spray. In the case of late injection at 300° aTDC, the spray penetration was initially comparatively shorter due to higher ambient pressure (~0.3–0.4 MPa). However, later, the spray plumes were blocked by the upward piston motion causing the wall wetting. For injection at 90° aTDC, at the middle of the intake stroke, the effect of strong intake flow was observed on the spray. It resulted in shorter spray due to dispersion of overall spray along with the surrounding flow. Soon, the spray collapsed as separate plumes were observed. An increase in the FIP resulted in considerable changes in the spray characteristics. It is easily noticeable from Fig. 7.5 that with higher FIP, the spray jet transitioned to an unstable form, resulting in finer spray droplets. Hence, their earlier evaporation was reported as no traces of droplets were observed after 4 ms of fuel injection. Another aspect noticed was related to the shape of the overall spray. Spray turned into rounder and thicker with increasing FIP. This was because smaller droplets at the spray tip experienced higher drag due to ambient, which easily spread out due to the following droplets.

Application of different alternative fuels resulted in variations in the spray breakup, droplet formation, and subsequent spray evolution owing to their different physical and chemical properties. In one such related study (Bao et al. 2014), experiments were conducted to evaluate spray penetration of different fuels, namely, isooctane, gasoline, and ethanol using Mie-scattering in an optical wall-guided GDI engine. Since the injector was side-mounted, hence image from the bottom presents the side view of the spray. The start of injection could not be viewed due to limited optical access in the piston crown. The spray penetration was obtained by considering the axial penetration of plume C, which was the highest among all the plumes. Spray penetration of ethanol was the lowest at a lower FIP of 40 bar. This was mainly

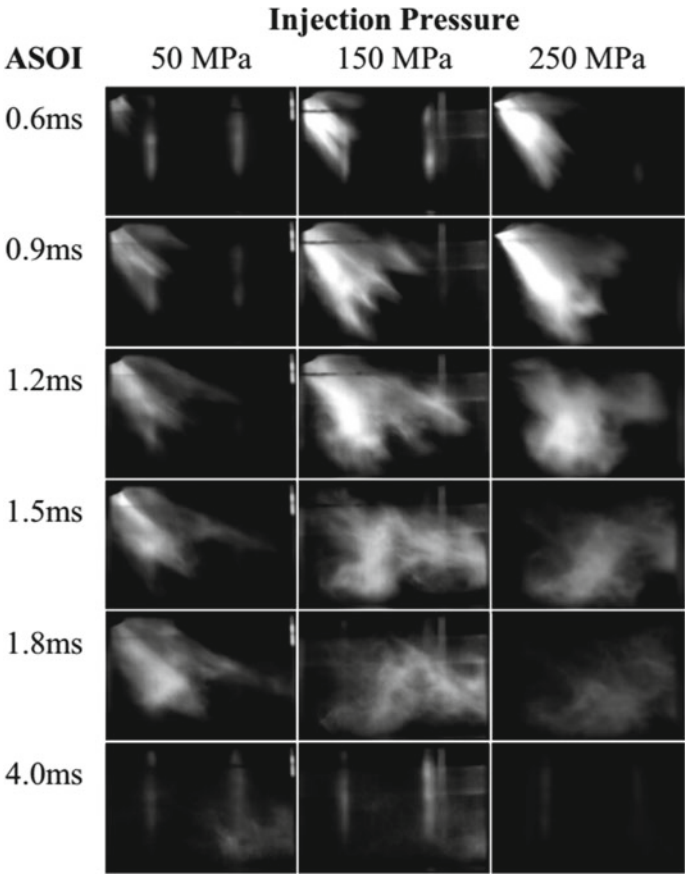

Fig. 7.5 Effect of FIP on spray development at SOI@ 90° aTDC (Song and Park 2015)

due to lower fuel injection velocity, owing to higher nozzle losses. Higher density of ethanol was mainly responsible for this. It can be explained by correlating with the expressions developed by Naber and Siebers (1996) for diesel spray penetration. As per this expression, spray penetration (S) is directly proportional to the velocity of the jet and time after the SOI (t), when time lies before the transition time of the breakup. After the transition time, spray penetration varies proportionally with the square root of the time after the SOI ($t^{0.5}$) and inversely to the ambient gas density. At lower FIP, spray penetration of all three test fuels varied with (t). Hence lower injection velocity for ethanol decreased with its penetration. However, at a higher FIP of 7, 11, and 15 MPa, the crossover between (S) $\propto$ (t) to (S) $\propto$ ($t^{0.5}$) was easily observed for all fuels. Here, spray penetration was mainly governed by the aerodynamic forces over the fuel droplets. Hence, ethanol spray reported the highest penetration for higher FIP due to its larger fuel droplets. In gasoline and iso-octane, smaller droplets suffered higher drag forces, which reduced their penetration.

Another study (Chan et al. 2014) investigated the structural transformation of gasoline and ethanol sprays undergoing flash boiling in an optical GDI engine. The results found that in the case of an early injection (~90° aTDC) when ambient pressure was low (~100 kPa), spray plumes showed higher convergence towards the injector axis, as shown in Fig. 7.6. This was mainly due to the flash boiling of spray as ambient pressure was lower than the vapour pressure of the fuel. On the other hand, for the late injection timing of 300° aTDC, spray plumes showed distinct features due to higher ambient pressure (~4 bar) than the fuel vapour pressure. However, FIP variation affected the structural transformation of the spray in both cases. With increased FIP,

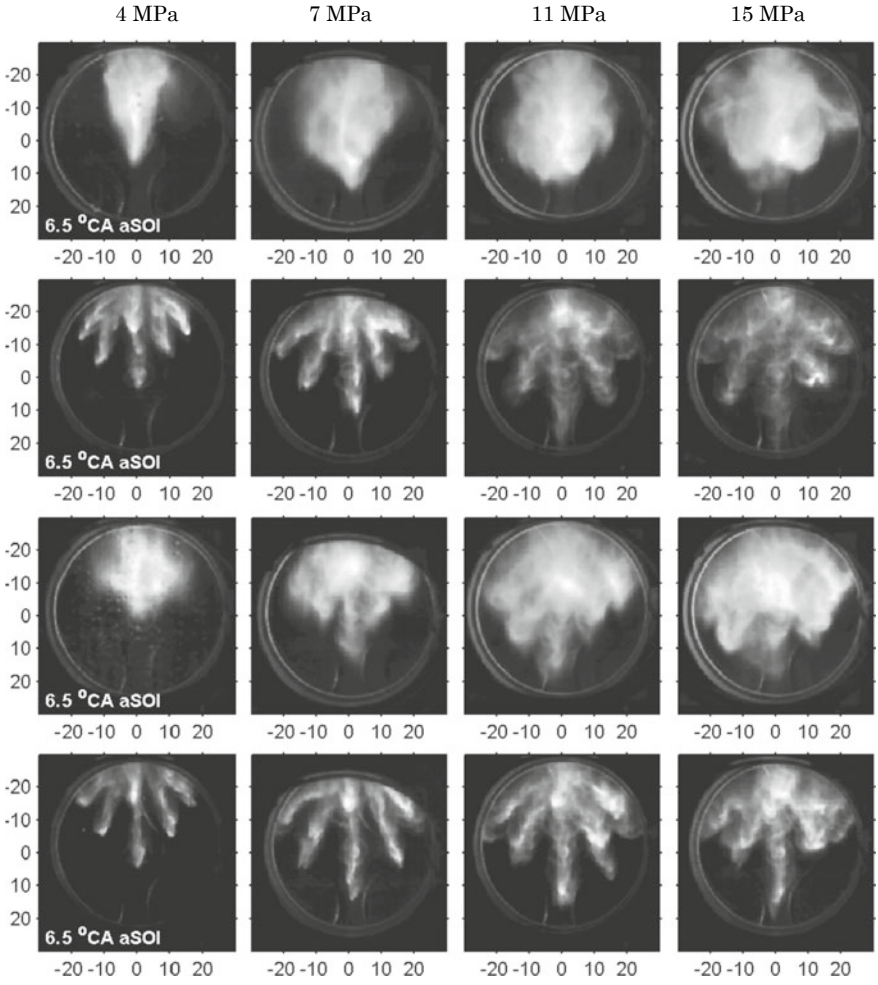

Fig. 7.6 In-cylinder spray images for different injections pressure. **a** Gasoline, SOI@ 90° aTDC, **b** Gasoline, SOI@ 300° aTDC, **c** Ethanol, SOI@ 90° aTDC, **d** Ethanol, SOI@300° aTDC (Chan et al. 2014)

flash boiling was less evident as higher spray momentum outperformed the spray convergence and imparted more directionality to the plumes. In addition, enhanced vaporization due to higher FIP was observed more for the flashing spray. Hence, the study suggested that both FIP and flashing conditions are suitable for providing a homogeneous mixture in the DISI engine. Further, gasoline and ethanol showed flash boiling based on the degree of superheating. For low ambient pressure, flash boiling of gasoline was more predominant at low FIP, while transitional flashing occurred at high FIP. For ethanol, transitional flashing at low FIP and no flashing at high FIP were observed. Overall, FIP on vaporization and flash boiling were more pronounced for gasoline due to higher superheating than ethanol.

In these above studies, optical measurements were obtained in a single-cylinder optical engine with a flat piston profile to maximize optical access to the combustion chamber. Hence, the measurements do not offer a complete picture of a commercial GDI engine. In that respect, a study performed by Catapano et al. used a multi-cylinder commercial GDI engine by converting it to optical configuration (Catapano et al. 2016). The engine had a wall-guided fuel injection system configuration. They incorporated elongated piston arrangement to allow optical access through the sapphire piston window located in the piston bowl. This was done such that it didn't affect the actual piston profile. The other optical access was provided by arranging an endoscopic probe through the cylinder head. This setup ensured minimal modifications to the structure to maintain the thermo-fluid dynamic configuration of a commercial engine. The setup arrangement is shown in Fig. 7.7. The endoscope used had a 70° angle wide field-of-view perpendicular to the tumble plane, including the injector and the spark plug.

For investigating microscopic sprays, the most common technique employed is Phase Doppler Interferometry (PDI). Almost all studies of microscopic spray characterization using PDI have been done in the Constant Volume Spray Chamber (CVSC). This doesn't consider the effects of in-cylinder flows or turbulence on the spray results and fails to simulate the actual engine-like conditions, though. On the contrary, the

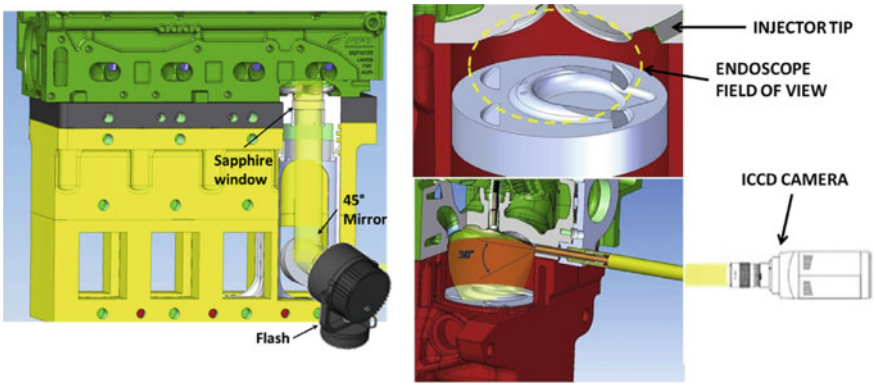

Fig. 7.7 Arrangement of endoscopy for spray imaging (Catapano et al. 2016)

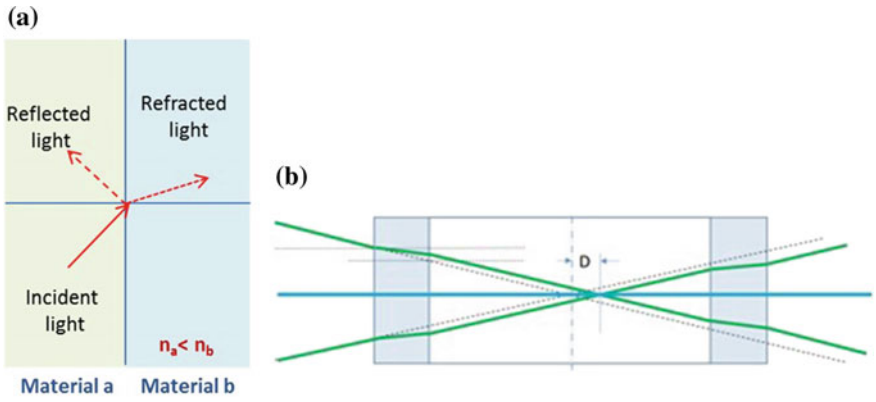

Fig. 7.8 **a** Phenomenon of reflection and refraction of laser beam passing through optical media. **b** Side view showing laser beams propagation (Sharma et al. 2020)

implementation of PDI on firing optical engines is a difficult task. For the first time, PDI was employed in firing optical GDI engine to study spray characteristics in real engine conditions at IIT Kanpur in our group. A comparative analysis was presented vis-a-vis results from the CVSC (Sharma et al. 2020). The most critical aspect in conducting the experiments was the alignment of laser beams through the quartz optical window, which was curved. For measurement accuracy, a pair of laser beams in the orthogonal planes coming from the transmitter must intersect at a common point called 'probe volume.' The procedure of attaining this is called the 'alignment of lasers.' The cylindrical quartz optical window caused difficulty in alignment due to the reflection and refraction of light due to change in medium. Hence, the best possible methodology adopted was to initially align the lasers using a similar surrogate window outside the engine and exact movement to locate the probe volume inside the engine w.r.t. the transmitter and the receiver.

Figure 7.8 shows how the presence of glass media refracts the incoming laser after reflecting a small (~15%) fraction. This is mainly dependent on the curvature, quality of the window, and laser beam quality. Considering a 2-component PDI system, one pair of lasers (blue) traverse horizontally, i.e., orthogonal to the cylinder axis. The other laser beam pair traverses in the vertical plane parallel to the cylinder axis. It was found that the direction of beams travelling in the horizontal plane was affected, while beams in the vertical plane suffered from refraction due to the angle of incidence. This was the case if the measurement point was at the center of the quartz window. However, for any other location, both laser beams showed slight refraction from their path. This study performed in-cylinder spray droplet diameter and velocity investigations in a firing optical GDI engine having a wall-guided spray system. The CVSC and in-cylinder engine experiments showed considerable differences in maximum spray droplet velocity components (V_x and V_y). In the engine experiments, maximum V_x and V_y were reported to be 29.8 m/s and 14.2 m/s, while in CVSC, they were 78.41 m/s and 23.92 m/s, respectively. The presence of dynamic temperature

and pressure conditions during engine operation led to a higher drag on the spray droplets, hence enhanced evaporation. Further, in-cylinder turbulence improved the mixing of surrounding air into the spray. In addition, higher ambient temperature reduced the surface tension of the fuel spray droplets. All these factors resulted in a reduction in droplet size, leading to loss of momentum and earlier evaporation before they reached probe volume. Therefore, lower maximum droplet velocity distribution was reported in the engine combustion environment. For a similar reason, spray droplets diameter distribution was also less scattered, and the bulk of droplets were in the range of diameter <10 μm in the engine experiments. This study demonstrated a comparative picture of transient and turbulent flows in the actual engine conditions w.r.t quiescent chamber. This dataset would certainly help improve the CFD models and provide more realistic results after model validation.

In addition to the wall-guided combustion system, several researchers also investigated spray evolution in the spray-guided combustion system. In one such study (Peterson et al. 2014), the laser was used for illumination. Figure 7.9 shows the spray images obtained from the Mie-scattered signals. Geschwindner et al. (2020) also used Mie-scattering for imaging. They used the diffused back illumination (DBI) technique in spray-guided GDI engines to capture the spray images, post-processed to evaluate the spray shape, penetration, and spray cone angle. ECN recommends DBI for liquid spray imaging.

The studies so far discussed used 2D planar imaging for liquid spray visualization in the engine. They have shortcomings when a complex 3D phenomenon is evaluated since out-of-plane motion with gradients are characteristics of the in-cylinder turbulent flows. However, with imaging technologies and optics evolution, 3D imaging techniques have come a long way. Chen et al. (2016) used a plenoptic imaging technique to capture 3D spray structure and its interactions with the surrounding flow under different operating modes in a spray-guided GDI optical engine. Baseline spray images under a quiescent environment were obtained to compare the effect of engine flows on the sprays. Studies were conducted for homogeneous and stratified charge modes, different engine speeds, and swirl ratios of the in-cylinder flows. Under homogeneous mixture conditions (SoI@300° bTDC), a strong intake-air flow was observed on the spray plumes trajectory. The impact of swirl momentum was quite prominent at a higher engine speed of 1300 rpm than 800 rpm. Decreasing the swirl ratio lowered the deviations in the spray plume directionalities. The spray structures varied significantly from cycle to cycle at higher engine speed and with a higher degree of swirl. For stratified charge preparation (SoI@35° bTDC), it was observed that apart from in-cylinder flows, the presence of high pressure and temperature also impacted the spray behaviour. The spray was susceptible to piston interactions. Images showed that the effect of swirl at both engine speeds on spray structures was minimal in stratified conditions. This is mainly due to reduced turbulence intensity and flow momentum as turbulence during the intake stroke dissolves during the compression stroke. Also, cyclic variations didn't affect the spray behaviour considerably. Hence, the spray was minimally affected as it was mostly driven by the spray momentum and not the flow momentum.

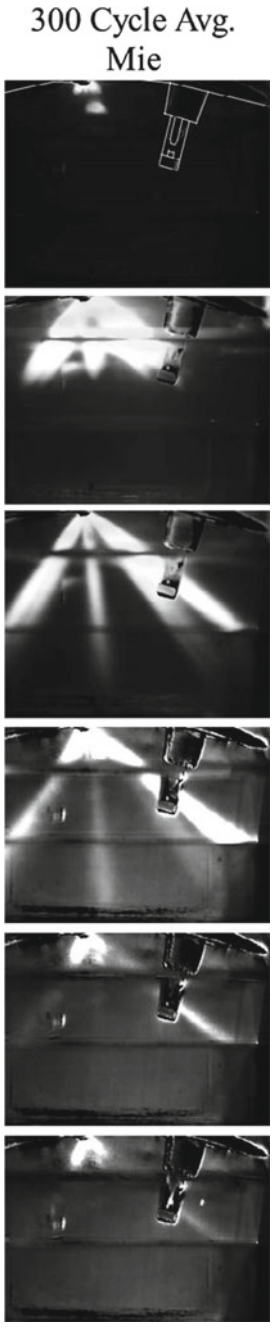

Fig. 7.9 Mie scattering images of fuel spray in a spray-guided DISI engine (Peterson et al. 2014)

7.2.2 *In-cylinder Flows and Spray-Flow Interactions*

Direct injections of high-pressure fuel can substantially change the in-cylinder flow behaviour via momentum exchange. Apart from large-scale bulk flow structures, it can influence small-scale turbulence too. In-cylinder flow mainly influences the mixing of fuel, air, and residual gases to alter the mixture quality. Further, ignition and early flame kernel growth are likely affected by the flow parameters near the spark plug. The rates of combustion and heat transfer also depend on flow turbulence. Hence, measurement of time-resolved flow-related parameters such as velocities, turbulent kinetic energy, dissipation rates, Reynold stresses, etc., are important for the engine design. To understand these phenomena for different fuel injection strategies, Clark et al. (2018) conducted a study to analyze the in-cylinder flows for five different fuel injection timing combinations. Double injection in a 1:1 split ratio was used for all five cases, and combinations were chosen from both timings in intake stroke to both timings in the compression stroke. The mean and fluctuating values of flow-field parameters were quantified using a novel spatial-filtering approach. Two spatial filtering approaches were considered, one based on fixed 8 mm cut-off length and another based on the cut-off filter length according to the mean flow speed at respective crank angle positions. The specifics of the methods used can be referred to in our other work (Clark and Kook 2018).

Experiments were conducted in a single-cylinder optical GDI engine with a multi-hole side-mounted injector. A PIV configuration was set up for swirl plane analysis, as shown in Fig. 7.10. The combinations of fuel injection timings used for double injection are listed in Table 7.1. These timings resulted in a wide range of mixture formation from well-mixed to highly turbulent. The image acquisition for PIV was in intervals of 42° to 28° bTDC, 5 mm below the fire deck. The upper limit was selected to avoid unwanted spray droplet signals, and the lower limit was selected so that the piston did not block the swirling plane.

The results showed that varying the fuel injection timing slightly resulted in significant differences in bulk in-cylinder flow behaviour and magnitude. However, 260–110° bTDC timing showed less bulk flow velocity despite a late injection. Further, it was noticed that the injection timing influenced the magnitude and direction of the tumble. A combination of 300 and 210° bTDC timing showed enhanced tumble flow, while reversal of tumble flow direction was observed at 300 and 110° bTDC and 140 and 110° bTDC timings. This could be a probable reason for low mean flow velocity in the case of 260–210° as flow induced by 2nd injection might be interfering with the flow caused by the first injection. In addition, cases having retarded injection timings resulted in higher TKE except for 140–110° bTDC timings. Cyclic variations in bulk flow structure were estimated by obtaining low frequency fluctuating intensity. A strong correlation was found between these fluctuations and the COV_{imep}. Although, cycle-to-cycle variations in TKE were not as per similar trends. Hence, it was suggested that the bulk flow parameter has a greater influence on the early flame growth than the turbulence. There was a likeliness of experiencing higher heat loss by the flame kernel to the spark plug electrodes in case of higher turbulence or

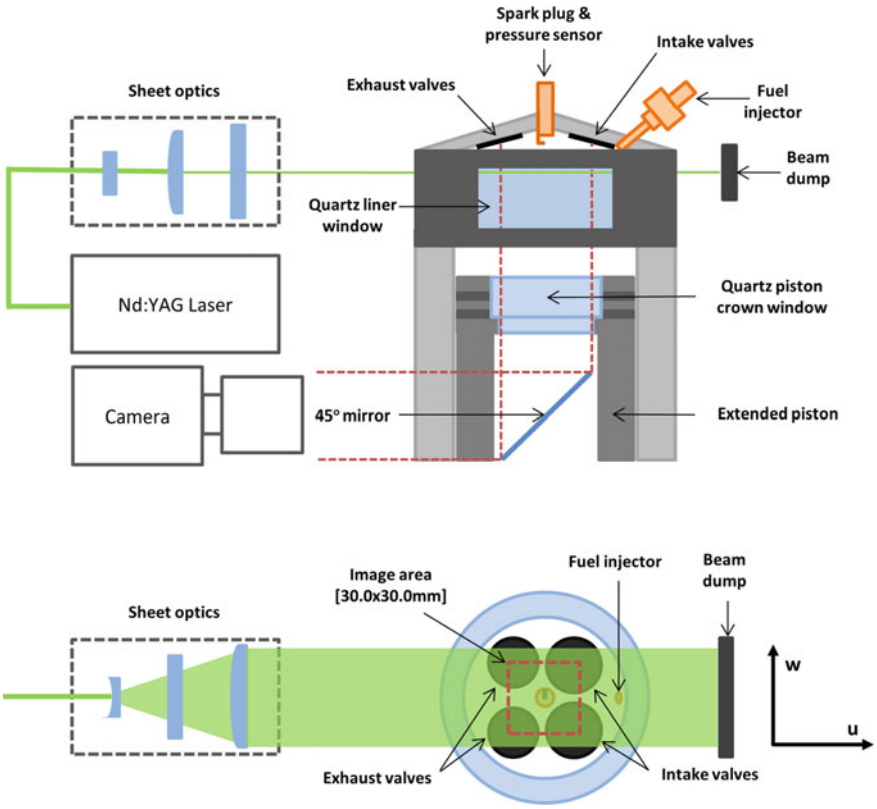

Fig. 7.10 Schematic of PIV setup for swirl plane analysis (Clark et al. 2018)

Table 7.1 Combinations of double injection timings (Clark et al. 2018)

Case 1	300 and 270° CA bTDC
Case 2	300 and 210° CA bTDC
Case 3	300 and 110° CA bTDC
Case 4	260 and 110° CA bTDC
Case 5	140 and 110° CA bTDC

small-scale flows near the spark plug. Also, integral length scales did not experience any significant changes with the injection timings with an 8 mm fixed cut-off filter. However, determining integral scales for engine flows is always a non-trivial task.

Researchers have also explored the potential of the combination of optical tools for a detailed and complete understanding of interdependent processes. In one such study by Stiehl et al. (2013), PIV and high-speed spray imaging were employed to investigate the mutual interaction of sprays and ambient flows in a spray-guided stratified DISI engine. The stratification was achieved by multiple fuel injections. The

results showed that the CCVs were higher for subsequent injections while the first injection was quite reproducible. This can be understood from Fig. 7.11, where the distribution of SH was quite larger for the 2nd injection. During the first injection, the flow field was mainly governed by bulk flow structures. The first injection transferred significant spray-induced turbulence to the flow field. As a result of shear forces occurring between spray and gaseous flow, two local toroidal vortices were generated, which increased the turbulence in the flow field locally, as shown in Fig. 7.12.

Hence subsequent injections in such higher turbulence levels with varying length scales were prone to get affected. Apart from this, rail pressure fluctuations after the first injection were also another major reason. Moreover, air-entrainment into the hollow spray during fuel injection caused due to the low-pressure region resulted in the upward airflow. This funnel flow varied in intensity and location, depending on the injection timing. For short delays between injections, the flow structures resulted

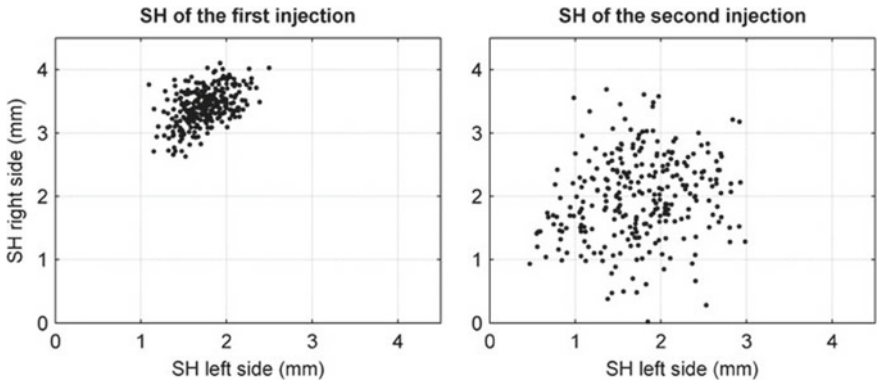

Fig. 7.11 Scatter plot of spray height (SH) of first and second consecutive injections (Stiehl et al. 2013)

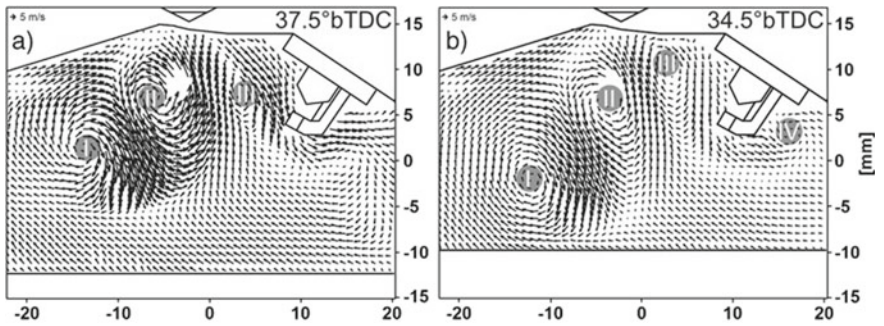

Fig. 7.12 Phase averaged flow fields for two instants between 1st and 2nd injection (Stiehl et al. 2013)

in high velocities, while for longer delays, it led to more stable spray due to early decay. Higher fluctuations were observed for the intermediate delays.

Similarly, another study (Geschwindner et al. 2020) investigated the interactions of bulk in-cylinder flows with late gasoline injection in two optical spray-guided engines. Testing on two optical engines offered different geometric configurations for the parametric study. The operating conditions of the experiment were following spray G standard condition of ECN. In-cylinder flow details were obtained using PIV, and Mie-scattering and DBI techniques were used for spray topology. Experiments were conducted for different inlet valve lifts and engine speeds. With the increase in both parameters, in-cylinder flow velocity increased. For quantifying the effect of flow field interactions with the spray, spatial probability maps for liquid spray were obtained, which showed the likeliness of liquid fuel presence. The results showed that spray outlines depicted broader probability distribution with ongoing injection events, indicating higher cycle-to-cycle variations. Also, cyclic variations increased for higher inlet valve lift and engine speed. It was found that higher in-cylinder flow velocities led to increased fluctuations in the spray G topology. Further, the penetration of spray was marginally affected by increased flow velocity. A slight reduction in spray expansion was observed for higher flow velocity. Also, increasing the engine speed and valve lift enhanced the upward recirculation of flow between the plumes. This restricted the spray collapse as plume-to-plume interactions were minimized. The spray-induced turbulence affected the ambient flow momentum significantly. It was hard to preserve the flow structures during injection in a weak tumble case, which yielded two counter-rotating vortices due to surrounding air entrainment. With high tumble intensity, most flow structures survived the disturbance caused by spray.

The intake manifold design for imparting specific in-cylinder flow structures is also widely studied by several researchers and is considered an important factor for optimizing engine performance. In a study by Stiehl et al. (2016), time-resolved PIV was implemented to investigate the effects of intake geometry on the in-cylinder flows and subsequent interactions with the spray. The experiments were conducted in a single-cylinder optically accessible GDI engine running in stratified mode. The engine had a spray-guided configuration with a hollow cone spray resulting from a piezo-actuated injector. Two modifications at the periphery of the intake port (S1, S2) were studied, as shown in Fig. 7.13.

The history of flow field evolution in the central tumble plane using time-resolved PIV helped determine the origin of flow structures and possible causes for their variations. The investigations were done for a stratified mixture prepared by triple injections in the late compression stroke. It was found that intake geometry variations significantly affected large-scale in-cylinder flow, causing deviations in tumble vortex position and strength. Further, the first spray injection was quite reproducible, while the second injection, which was mainly responsible for forming an ignitable mixture, exhibited significant fluctuations. Fluctuations in the spray shape were quantified by SH, which was defined as the vertical distance from the spray plume boundary to the cylinder head. Variations in SH of 2nd injection were correlated with regions showing large cycle-to-cycle flow field variations. However, the variations in 2nd spray were similar for both port geometries, despite substantial differences in their flow fields.

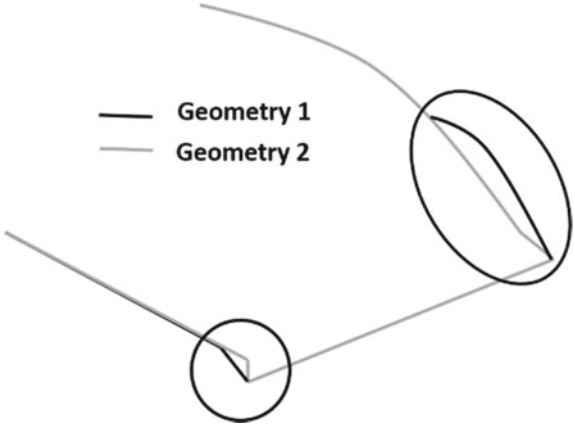

Fig. 7.13 Inner contours of geometric variations of the intake port (Stiehl et al. 2016)

This showed that spray fluctuations were insensitive to geometry changes. For both port geometries, the first injection-induced upward flow field near injector tip due to formation of a low-pressure zone within hollow spray cone. The tracing of the time history of the flow field for geometry G1 using correlation analysis revealed that variation in positions of large-scale tumble vortex from cycle-to-cycle during intake was a major reason behind 2nd spray fluctuations. In addition, turbulence induced by 1st spray injection sought to increase the impact of flow cyclic variations on 2nd spray fluctuations. Further, their correlation decreased in the central tumble plane while tracing backwards towards the intake process. This could be mainly because of the out-of-plane flow, which was highly prevalent in G2 geometry. Tomographic or multi-plane PIV can overcome this limitation of planar or 2D measurements.

Stratified operation in spray-guided engines involves close coupling between the fuel injection and the ignition events. The developing ignition kernel gets subjected to steep gradients of fuel concentration and flow velocity. Hence, in such conditions, the likeliness of variability from cycle to cycle is higher. These unfavourable fluctuations can impact the combustion quality because of misfires and partial burn cycles. Hence, engine control parameters should be optimized for stable and sustained stratified combustion. In this regard, in-cylinder flow evolution and its cyclic variability are critical factors to consider.

Further, the intensity and behaviour of intake flow can impact the turbulence and flow structures resulting from spray-air interactions, impacting the repeatability of fuel–air mixing. In a study by Zeng et al. (2016), intake generated swirl flow resulted in more repeatable and stronger vortex formation in the piston bowl because of the interactions of injected spray plumes from the multi-hole injectors than without swirl generated flows. The injection of liquid fuel spray redistributes the momentum of the gas phase such that it leads to a stronger and repeatable vortex. The formation of this vortex promoted effective combustion with fewer cyclic variations.

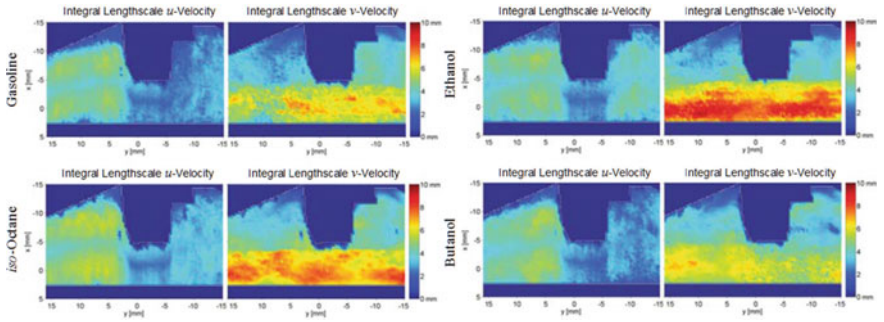

Fig. 7.14 Integral length scales in tumble plane for different fuels (Aleiferis and Behringer 2015)

Studies have also been attempted to categorize the flow characteristics for different kinds of fuel injection. Researchers characterized the in-cylinder flow in one such study and quantified the integral length scales associated with turbulence for different fuels (Aleiferis and Behringer 2015). They considered the effect of gasoline, isooctane, ethanol and butanol injection on the flow field at the time of ignition using PIV. A single-cylinder optical research engine having a side-mounted swirl-type DI injector was used for the study. Experiments were conducted for stoichiometric homogeneous mixture preparation (~60° aTDC) and at a fixed engine speed of 1500 RPM. For without injection runs, mean flow velocities of the order of 3–5 m/s and TKE between 9 and 15 m^2/s^2 were obtained for tumble plane from intake to exhaust. Two counter-rotating vortices were observed beneath the two intake valves in the swirling plane, having flow magnitude similar to that of the tumble.

However, fuel injection during intake didn't cause significant changes in the flow field at the time of ignition. For gasoline, flow velocities were 10% higher, while it was reduced by 30% for butanol and ethanol and isooctane were in-between these. Further, injecting the fuel shifted the highest TKE zone from the exhaust to the intake side. The integral length scales for both fuel-injected and without fuel-injected cycles came in the same order of magnitude for the tumbling plane while showed slightly higher values for injected cases in the swirling plane. Non-dimensionally, these scales were ~20% of the clearance height and 5–12% of the bore. Fuel types didn't result in large differences as average scales were in the range of 4–6 mm in both planes. Specifically, the largest scales were associated with ethanol and the smallest with butanol, as shown in Fig. 7.14.

7.2.3 Fuel–Air Mixture Formation

The most intense application of optical measurement in engine research is fuel–air mixing quantification. These are mainly performed by laser-induced fluorescence imaging or absorption techniques via the use of laser diodes. Traditional PLIF works

by capturing fluorescence signals emitted by selected tracer upon getting illuminated. Tracers follow the path of fuel droplets, which have to be selected such that they are a close surrogate to the actual fuel and do not emit fluorescence. Otherwise, there would be interference of signals and may affect the gasoline results. Isooctane is used as a surrogate to gasoline due to its similar boiling point. However, isooctane, a single component fuel, cannot represent the actual evaporation characteristics of gasoline, a multicomponent fuel. In the GDI engine, the injected fuel is present in both liquid and vapour phases. Due to differences in emission intensity between liquid and vapour phases of the fuel, it becomes difficult to obtain accurate results. The laser-induced exciplex fluorescence technique (LIEF) uses filtering methods to separate the wavelength spectrum from both liquid and vapour phases to overcome this challenge. Various studies have shown its successful implementation and a detailed experimental setup procedure (Ipp et al. 2000; Kang and Kim 2003; Deschamps et al. 1999). Most studies based on LIF use dopant tracers representing similar evaporation characteristics to the test fuel. However, the real fuel comprises hundreds of distinct hydrocarbon components, with preferential evaporation.

The evaporation of lighter components takes place at different timing compared to heavier ones. For investigating preferential evaporation of multi-component gasoline, 2-tracer LIF is used in many studies. In a study by Bardi et al. (2019), 2-tracer LIF was used, and preferential evaporation was examined for ethanol-blended gasoline. It was observed that with a lower fraction of ethanol blending (E20), evaporation of ethanol took place earlier than iso-octane. This was expected due to the lower boiling point of ethanol. However, for a higher fraction of ethanol blending (E85), ethanol evaporation occurred after isooctane and n-pentane. Moreover, ethanol formed an azeotropic mixture with isooctane and n-pentane due to their higher chemical and physical affinity.

The stratification in wall-guided configuration is very difficult to optimize for a wide range of engine operations. This was mainly due to the shortage of time available for mixture preparation. It involved the transport of fuel in the vicinity of the spark plug via piston cavity. The fuel–air mixture distribution near the spark plug is a critical parameter of the study, as it determined the early flame development and following combustion behaviour. Hence it was crucial to investigate the equivalence ratio of the mixture near the spark plug at the time of ignition. In one such study by Deschamps et al. (1999), two techniques, (i) Combined Catalytic Hot Wire Probe and (ii) LIEF, were used to obtain the mixing characteristics in a stratified mixture. Experiments were conducted for different late injection timings (60–30° bTDC) and different lean mixtures with global Φ varying from 0.3 to 0.6. Both these techniques showed rich mixture cloud at the time of spark near the spark plug. However, it was observed that an increase in the injection duration did not affect the maximum equivalence ratio of the mixture in the vapour cloud. Instead, it caused an increase in the size of the rich vapour cloud. Lean mixture with late injections showed large cycle-to-cycle variations in LIEF measurement compared to homogeneous mixture preparation. Steeper and Stevens (2000) also performed a mixture preparation study using LIF for different injection timings in an optical spray-guided engine. They used gasoline fluorescence for qualitative visualization of vapour phase gasoline.

The measurements were done in a horizontal plane 13 mm below the spark plug at the time of the spark. The results showed an increasing degree of heterogeneity in vapour distribution with respect to the retarded injection timings. A similar trend was evident from the higher CoV of the light intensity distribution. In another study related to the effect of injector fouling, mixture formation was studied using PLIF in a spray-guided DISI optical engine using a fouled injector (Badawy et al. 2018). This study was conducted with isooctane as surrogate fuel and a 3-pentanone (3% w/w) dopant tracer. The PLIF images were captured at 30° bTDC, which was considered ignition timing in the combustion tests. The experiments were performed at a fixed engine speed of 1200 RPM under motored conditions and 150 bar FIP. The PLIF images obtained for choked and clean injectors at varying injection timings are shown in Fig. 7.15. The SOI of 320 and 280° bTDC resulted in a fairly homogenous mixture distribution having Φ in the range of 0.9–1.2. The spatial variations in fuel concentrations were minimum due to greater time availability for almost complete evaporation. Slightly retarding the injection timings to 240 and 200° bTDC resulted in higher inhomogeneity in the mixture (Φ ~ 0.9–1.3), which was further enhanced in the choked injector (Φ ~ 1.4–1.8).

These characteristics were the main reasons for higher particulate emissions. With later injection timings (160 and 120° bTDC), both injectors obtained substantially rich fuel concentrations on the left zone of ROI (near exhaust valves). This was mainly due to the bulk convection of unevaporated fuel in the tumble direction. For further investigating the cyclic variability in charge formation, COV of spatial light intensity distribution (SLID) was measured for each case. Evaluating this showed poor mixing characteristics for choked injectors due to the higher COV of SLID. Also, for both injectors, variations increased with retarded injection timings. Stratification in GDI engines is critical due to the transient nature of the flow field during the engine operation. Design parameters are required to be optimized for the formation of required mixture stratification at different engine operating conditions. Intake manifold geometry and piston shape play a key role in determining the flow pattern in the combustion chamber. The authors investigated different designs for understanding their effects on the mixture formation. In a study by Kang and Kim (2003), different piston shapes and intake flows were investigated for stratified DISI engines having centrally mounted swirl injectors. LIEF was used for obtaining the fuel distribution. Three piston shapes were considered for this study, having flat, bowl and re-entrant shapes. It was found that tumble flow resulted in faster evaporation than swirl flow for early injection timing (270° bTDC). For early injection, a tumble flow caused fuel vapour distribution in the lower region of the combustion chamber. In the case of late injection (90° bTDC), it caused the movement towards the intake valve side. For swirl flow, the mixture was mainly concentrated near the central region in the bowl piston while it was distributed towards the exhaust valve side in a flat and re-entrant piston. A re-entrant piston with injection timing of 60° bTDC was better for stratification due to the smaller bowl diameter. The likeliness of cycle-to-cycle variations was also high in the stratified mode of combustion in DISI engines. These CCVs were mainly due to differences in mixture formation and quality of the combustion cycle. Higher occurrence of partial combustion and misfire generally enhanced the CCV of the

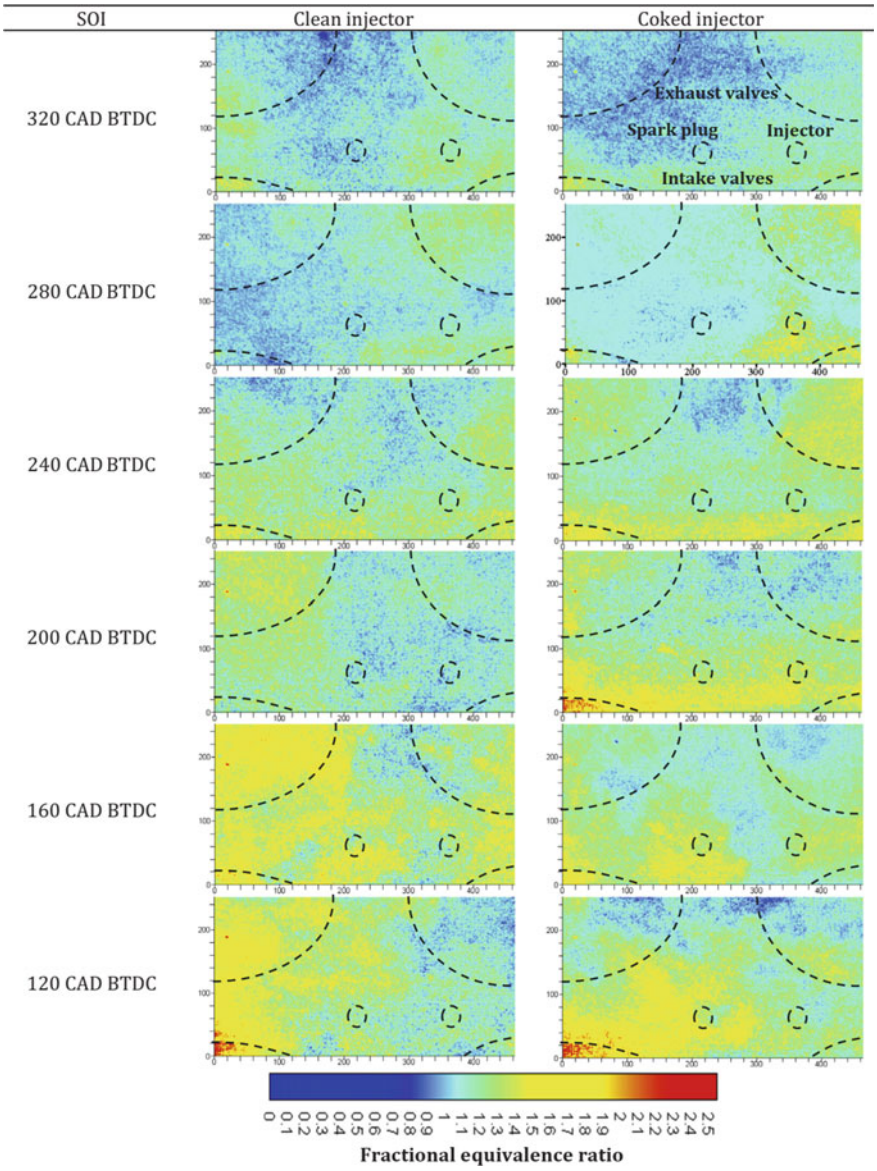

Fig. 7.15 Equivalence ratio distribution using PLIF for injection timing sweep for clean and choked injectors (Badawy et al. 2018)

imep. There is no universal reason for such poor combustion cycles. There could be multiple reasons, such as over-rich or over lean charge, inadequate flow velocities, or fluctuations in ignition energy. Researchers have widely used optical diagnostics for investigating the reasons for misfires and high CCVs. In one such study by Peterson et al. (2011), PIV and PLIF techniques were used for understanding the flow and fuel distribution at the time of ignition for partial burn and misfire cycles in a spray-guided stratified GDI engine operation. The results showed that these cycles were generally associated with lean mixtures and low flow velocities near the spark plug. However, there were well-burning cycles also having low flow velocity and equivalence ratio. Deeper investigations revealed that the ignitable mixture formed near the spark plug, but the flames failed to propagate towards the bowl with fuel-rich zones. Hence, the late arrival of the flame kernel and subsequent surrounding leaner conditions led to failed flame propagation.

Further investigations (Peterson et al. 2014) revealed that major factors responsible for slower flame development were the presence of lean mixtures, dilution of charge by EGR, and unfavourable convection of flame kernel away from the flammable charge due to upward flow. Managing flow to obtain desirable fuel–air mixing is important to enhance combustion stability in stratified DISI engines. Studies have found that intake-generated swirl is beneficial in spray-guided configurations for repeatable mixture formation during early frame growth (Zeng et al. 2016, 2015). However, on the other hand, a strong swirl has shown a detrimental effect (Drake et al. 2005). The authors also investigated the interactions of swirl and tumble dominated flow fields with sprays. These findings are described in our previous chapter (Kalwar and Agarwal 2021). In another study (Zeng et al. 2017), the authors evaluated its impact on gasoline vapour distribution using high-speed infrared (IR) imaging of C-H band emitting wavelengths. It was found that both swirl and tumble dominated flows led to asymmetric distribution of gasoline vapours in the later part of the compression stroke. These regions were also correlated with high soot luminosity. Symmetric and uniform distribution of fuel vapour was observed for the no-swirl case.

To limit the exhaust CO_2 emissions, downsizing of GDI engines is essential. At the same time, boosting is done to compensate for the power loss by engine downsizing. However, the performance of these engines is limited by increased knock or pre-ignition tendency. Researchers investigated Octane on demand (OOD) concept to resolve this, where two fuels with different RON are injected in the dual-injection mode. Base fuel with low octane numbers such as Naptha and the octane boosters such as ethanol is injected using optimized injection strategies to maintain the desired RON, depending on the engine operating conditions. Pilla et al. (2016) conducted experiments to evaluate the fuel concentration and mixing processes for three different dual-injection strategies (port + lateral), (port + Central) and (Central + lateral) using 2-colour PLIF. The measurements were done in motored engine conditions, having SOI at 260° bTDC.

The PLIF images were captured at 60° bTDC in the vertical plane. They reported that the injection strategies did not affect the fuel repartition in the combustion chamber. Hence it was mainly dependent on a single injection having negligible

interaction between the spray plumes. The single injection from the central injector accumulated the fuel near the piston top and on the right side of the liner near the exhaust valves. For injection from the lateral injector, the fuel presence was mainly on the intake side of the liner and lower right zone near the walls. Direct fuel injection in the SI engine also benefits the charge cooling, an important parameter considered during mixture formation. It enhances volumetric efficiency and avoids preignition in the downsized engine. In a study by Attar et al. (2014), the thermometry technique was successfully demonstrated by tracer-based 2-line PLIF to evaluate the charge cooling due to fuel injection. The results obtained were in agreement with the calculations of temperature from the pressure data. The study suggested that both injection quantities and timings influenced the charge cooling. Charge cooling happens when the injected fuel evaporated by absorbing heat from the surrounding air. Hence, increasing the fuel injection quantity led to an increased cooling effect. Late injection timing (250° aTDC) reduced the in-cylinder temperature by a higher amount than earlier (90° bTDC). This was mainly due to the opening of the intake valve during the early injection. Hence, the enthalpy of vaporization allowed greater air mass to enter the cylinder. On the other hand, for later injection timings, the evaporation occurs for a fixed air mass as the inlet valve closes. The authors reported a 50% increase in the charge cooling when injection timing shifted from early to late injection for a low fuel injection quantity. Although for higher fuel injection quantity, the rise was only 10% due to the fuel impingement. Though in-cylinder temperature measurement (thermometry) is performed by various techniques such as LIF, Coherent anti-stokes Raman scattering (CARS), or Rayleigh scattering, these methods result in low accuracy. The authors demonstrated a laser-induced thermal grating system (LITGS) for more precise measurement of in-cylinder temperature in a range of 0.1–1% (Williams et al. 2014). This can also resolve the issue of high CCVs in the temperature measurements. LITGS uses signal's frequency, whereas other techniques use signal intensity. Hence, it remains unaffected by noise.

7.2.4 Flame Evolution and Pollutant Formation

Optical combustion and flame development investigations are generally performed using various techniques, such as natural flame luminosity, chemiluminescence imaging, emission spectroscopy, and LIF to detect plasma and unburnt charge characteristics, etc. In homogeneous charge preparation, combustion processes are similar to carburetted or port-injected SI engines. While for late injection, heterogeneous and stratified mixture presence near the spark plug offers difficulties in combustion due to highly rich or highly lean mixture. A highly turbulent flow can affect ignition stability. Hence, it is important to study the combustion in GDI engines as a possible combination of premixed, partially premixed, or even non-premixed charge. The following paragraphs discuss research studies that investigated the effect of fuel injection parameters on combustion and flame characteristics via high-speed imaging. In a study by Lee et al. (2020), combustion images for various fuel injection

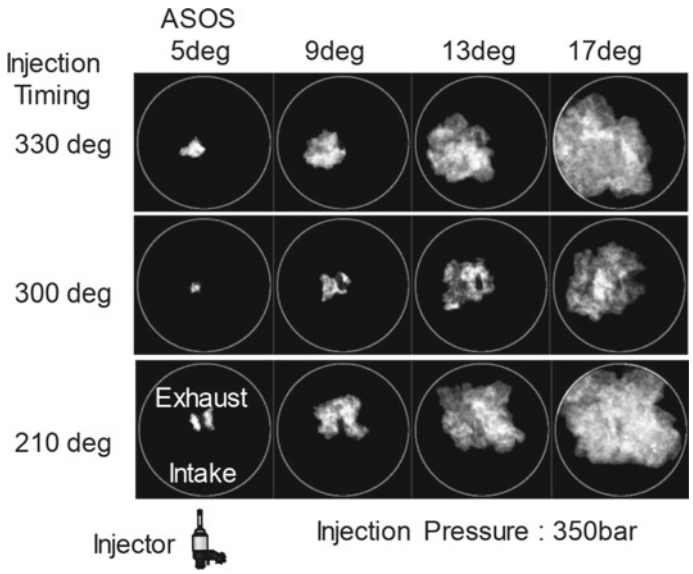

Fig. 7.16 Images of flame propagation for various injection timings (Lee et al. 2020)

timings were obtained from an optical GDI engine with the side-mounted injector. Initial flame growth was slower for early injection timing (~300° bTDC) than in the other cases, as seen in Fig. 7.16. This slower flame development was mainly due to weaker in-cylinder flows due to injected fuel and the in-cylinder airflow in the opposite directions. Further, the flame center movement was obtained for different injection timings, indicating bulk in-cylinder airflow. The movement of the flame center in the direction of fuel injection took place as the injection timing was retarded, as shown in Fig. 7.17.

In another study, it was observed that compared to early injection, late injection showed faster initial flame propagation due to presence of a locally rich mixture around the spark plug (Clark et al. 2014). Hence, in addition to global equivalence ratio or mixture properties, local conditions also play a significant role in the subsequent combustion processes. They also reported that advancing the ignition timing increased the flame speed. At early ignition timing, higher piston speed maintained a higher TKE of the ambient airflow. The overall combustion process of the stratified mixture was observed to have both lean premixed and mixing controlled combustion (Oh and Bae 2013). Non-luminous flames for early injections mainly resulted from over-mixing of charge, while sooty luminous flames for late injections were due to under mixing of charge. In a study by Song et al. (2018), it was found that increasing the FIP from 50 to 500 bar reduced the fuel film over the piston for injection timing of 210° bTDC, as shown in Fig. 7.18. They reported that at a lower FIP of 5 MPa, a change of injection timing from 330° bTDC to 270° bTDC resulted in a considerable reduction in particulate emissions. In contrast, at 50 MPa FIP, this change was negligible.

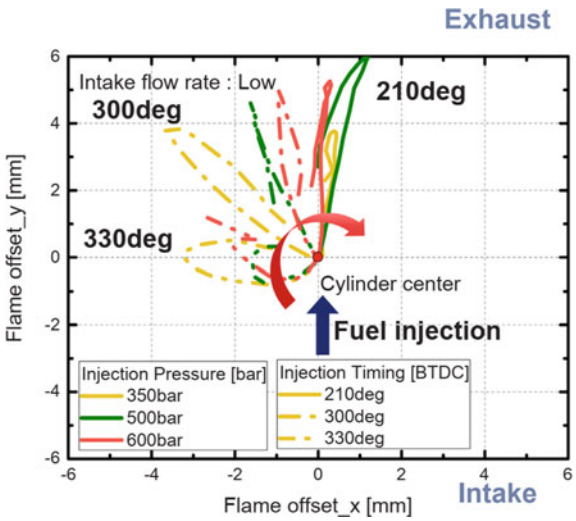

Fig. 7.17 Variations of flame center travel for different injection timings (Lee et al. 2020)

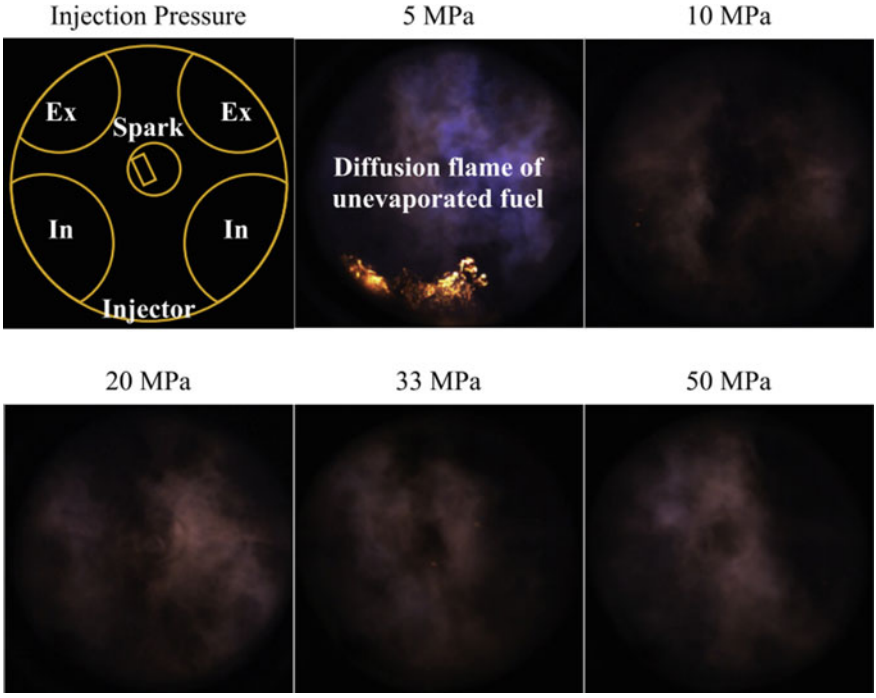

Fig. 7.18 Flame images for different FIP after 52° SOS (Song et al. 2018)

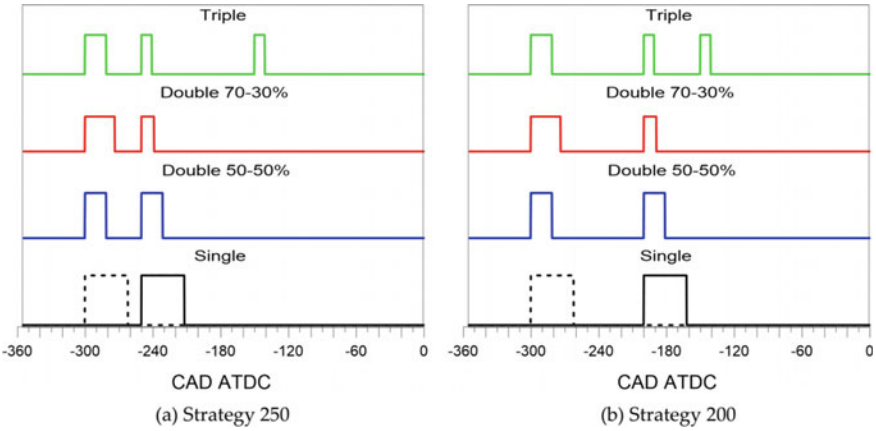

Fig. 7.19 Details of injection strategies adopted w.r.t. 2nd injection position. **a** 250° bTDC, **b** 200° bTDC (Martinez et al. 2019)

Injection strategies are important tools that define mixture formation and optimize the engine for higher performance with lower emissions. Several authors investigated multiple injection strategies. In a study by Martinez et al. (2019), the effect of single, double and triple injections was investigated for different split ratios and injection facing the wall guided optical engine, as shown in Fig. 7.19. and soot emissions obtained with the splitting of injections.

Figure 7.20 shows flame images from the double injection strategy. It can be concluded that splitting the injection with retarded second injection resulted in a lower luminosity than baseline early injection. However, with the late second injection, flame growth was delayed for both single and double injections. This shows that the combustion is improved for the split cases. Similarly, triple injection also exhibited similar behaviour. Overall, double injection with a 70:30 split ratio gave the best results. The authors concluded that flame propagation became less sensitive to injection facing than a single injection with split injection. The Heywood circularity factor (HCF) was obtained, which indicated distortion in the flame shape. Figure 7.21 shows that the HCF increased with retarded injection facing and decreased with multiple injections. Also, single injection led to the preferential direction of flame propagation towards the exhaust valve, while, for multiple injections, flame propagation was more uniform. Hence, these observations presented the basis for lower cyclic variations.

In another study, the authors investigated the effect of injection strategies on flame characteristics and propagation for a side-mounted injector equipped GDI engine (Song et al. 2015). The authors analyzed a single injection strategy with different injection timings during the intake stroke and a double injection with a short second injection at the end of the compression stroke. Figure 7.22 shows the flame images for the single injection strategy. It was observed that flame speed slowed down with the advancing injection timings.

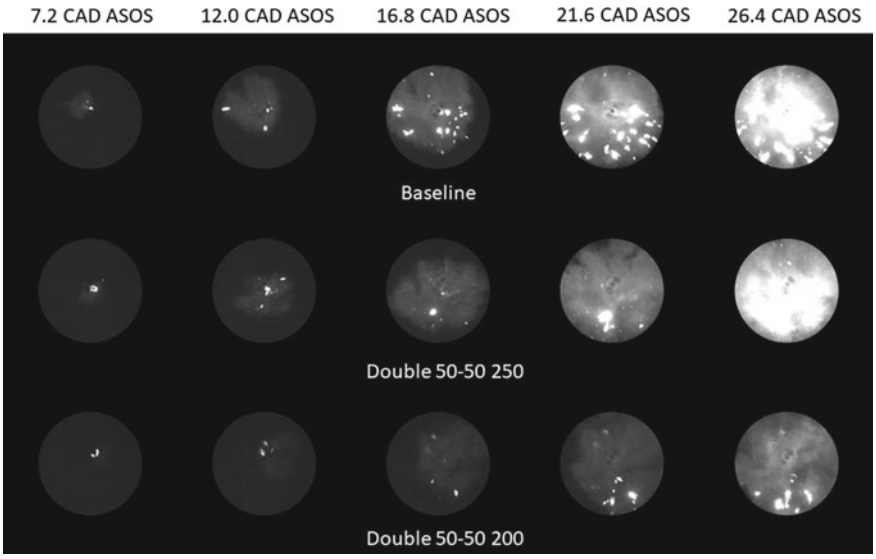

Fig. 7.20 Flame images for single (baseline) and double injection strategy (Martinez et al. 2019)

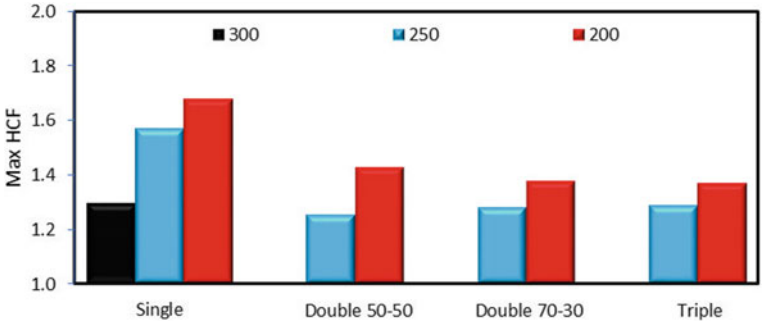

Fig. 7.21 Heywood Circularity Factor (HCF) for different injection strategies (Martinez et al. 2019)

Late injection timings led to higher peak pressure and faster flame propagation due to enhanced in-cylinder turbulence. Injection timing of 180° aTDC resulted in a flame speed of 20 m/s (55 times that of gasoline laminar burning speed), while 0° aTDC injection timing resulted in the slowest combustion with the flame speed of 10 m/s. 80% of fuel was injected during the intake stroke (~45° bTDC) in the double-injection strategy, while 20% was injected later at different timing. From Fig. 7.23, it can be observed that injection timing of 35° and 45° bTDC resulted in similar flame characteristics.

For both injection timings, bright yellow diffusion flames were observed during early frame growth due to the combustion of liquid fuels. Further flames interacted with fuel impinged on the piston, which was observed as a pool fire. Piston wetting

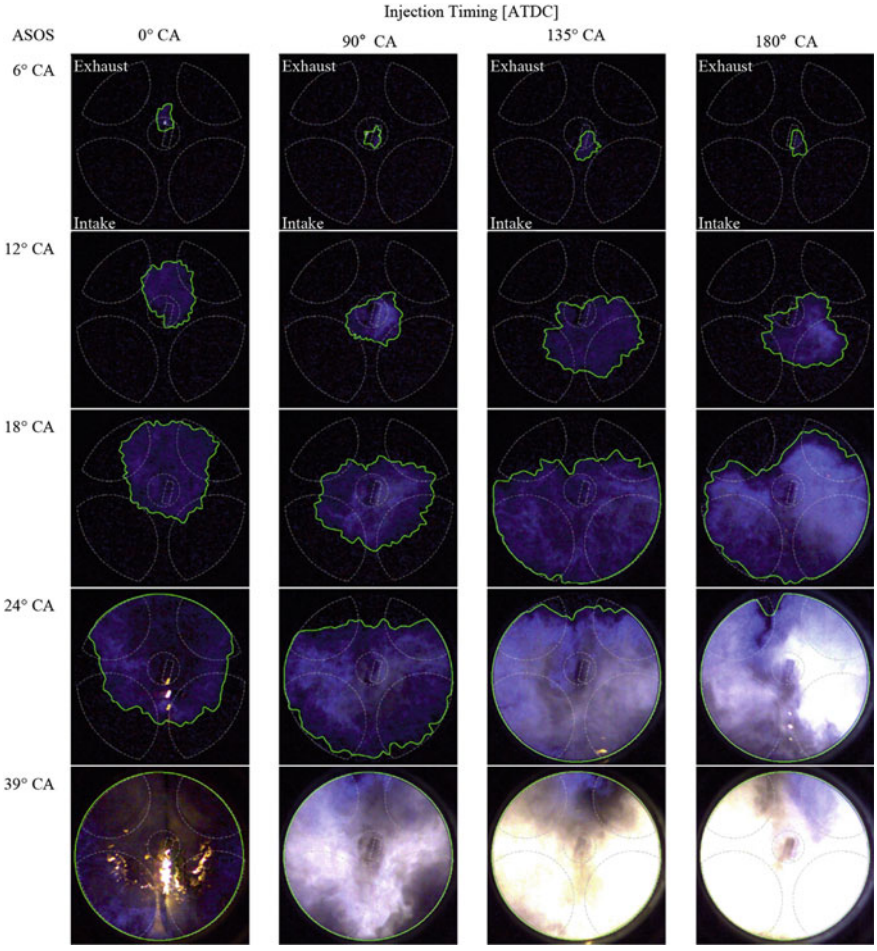

Fig. 7.22 Flame propagation images for single injection strategy having different injection timings (Song et al. 2015)

is unavoidable in the wall-guided configuration, and it is a major source of soot formation. However, 50° bTDC injection timing showed very slow flame propagation due to lack of combustible mixture. These observations correlated with the peak combustion pressure as 35° and 45° bTDC resulted in higher peak pressure than 50° bTDC. Flames propagated towards the exhaust valve for early injection, while the flames moved towards the intake valve for late injections. These were mainly dependent on the presence of combustible mixture.

Similar observations were reported in the study conducted by Clark et al. (2016). They found that double injections resulted in more spherical flame while single injection led to elliptical flames. The eccentricity of the flame front was not affected by the equivalence ratio variations. Close alignment between the semi-major axes of

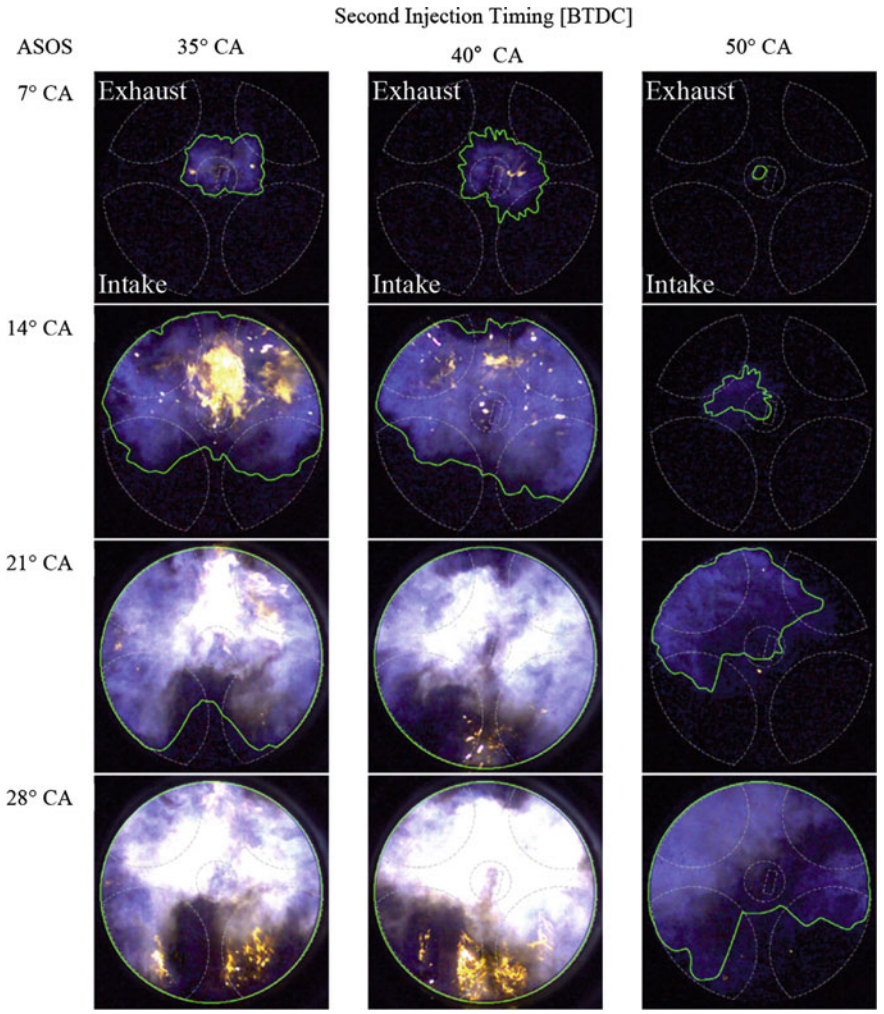

Fig. 7.23 Flame propagation images for double-injection strategy having different 2nd injection timings (Song et al. 2015)

the elliptical-shaped flames and the fuel jet path in the direction of the tumble was observed for both strategies. Wrinkling of the flame front was observed for both injection strategies, which implied that wrinkling was mainly an outcome of turbulence effects and was not affected by the richness or leanness of the mixture. Regardless of the second injection was positively correlated with the eccentricity of flames due to decreased charge homogeneity (Clark et al. 2017). Marseglia et al. (2017) observed that the main flame front exhibited asymmetric and heart-shaped geometry. For single injection, the concavity of flame front was towards the intake valve side, while that for split injection, it was towards the exhaust valve side. The highest knock occurrences

were concurrent with the zones having residual charge susceptible to auto-ignition before consuming the flame front. CFD simulation results supported the observations from optical combustion engine experiments. TKE distribution was higher for single injection, asymmetrically, along with the flame front propagation. In addition, equivalence ratio distribution also guided the flame speed and flame movement. Overall, the split injection was advantageous in reducing cyclic variations and knock propensity, improve combustion efficiency, and reduce undesirable pollutants.

Lean mixture combustion in DISI engines is widely researched due to its thermal efficiency and fuel economy benefits. Its advantages are mainly obtained during part-load conditions due to reduced pumping losses. However, leaning the mixture is limited by acceptable cycle-to-cycle variations due to combustion instability. Flow control for proper fluid motion can be beneficial in compensating the reduced mixture reactivity by enhanced turbulence level. Stratification of the mixture by late injection offers combustion sustainability at the overall leaner mixtures. Though, it leads to diffusion flames due to wall impingement, resulting in higher PM emissions. For greater insights into lean mixture combustion and their flame characteristics, Irimescu et al. (2018) conducted flame imaging for lean mixtures at different equivalence ratios in a wall-guided optical engine. This provided more valuable information about the spatial distribution of burned species and interactions with the in-cylinder airflow. They also analyzed the effect of the start of injection and engine speed on the combustion characteristics. The crankshaft rotational speed of 1000 rpm allowed maximum dilution ($\lambda \sim 1.6$), and 2000 rpm allowed the least dilution. Results showed that flames were generally directed towards the exhaust valves with similar overall flame intensity for stoichiometric mixture at different engine speeds. Higher wall temperature region towards that part along with tumble could have led to this. Slower flame evolution ($\lambda \sim 1.3$) with inherent offset for the engine speed showed a prolonged initial phase as the underlined factor. Although, combustion velocity was quite similar in fully established turbulent flame propagation. Higher luminous intensities were observed during late combustion, attributed to chemiluminescence of premixed combustion and soot particles formation during diffusion-controlled combustion. It was reported that diffusion flames mainly originated from two sources. First, from the oxidation of liquid fuel film over the piston, the second was associated with the unburned gas returning from the piston top (jet-like flames). Diffusion flames were for all cases, where luminosity at the intake region was quite repeatable. This could be due to the presence of fuel impingement from a vertical plume from the injector. Speed of 2000 rpm led to more distributed intensity due to the tumbling effect. However, the time dependence for both cases was different, which affected the chemical kinetics. The liquid film over the piston was consumed by propagating a premixed combustion flame for the first case.

In contrast, flame propagation was almost over for the second case when the unburned gas returned from the top land region. Hence, the latter type of flames were found near the exhaust valve side with lesser repeatability. Also, the diffusive flame area for $\lambda \sim 1.3$ was smaller than for $\lambda \sim 1$, which correlated well with the smoke opacity. For further details about the chemical nature of reactive flame species, spectroscopic analysis was done at the intake valve and exhaust valve side.

At 60° CA after ignition, detection of OH radicals (~310 nm) indicated fuel oxidation even during late combustion. However, their presence was found where diffusive flames are absent, which could be associated with a high-temperature zone in the premixed combustion. At 70° CA after ignition, high wavelength emissions were observed for both locations (2 and 7), which indicated the presence of a carbonaceous structure. The engine speed of 1000 rpm recorded higher soot compared to 2000 rpm. For different injection phasing (340°, 300°, 260°), it was observed that both early and late injection timing resulted in the higher displacement of flames. These were mainly a result of charge stratification and flow motion generated due to interactions of spray jets. 300° CA was found to be optimum with a reduced flame shift. The authors concluded that the fuel injection timing for lean limit would be optimized for stoichiometric combustion. Martinez et al. (2017) investigated flame characteristics of fuel–air mixture with different air–fuel ratios (from $\lambda = 1$ to $\lambda = 1.6$) in a wall-guided GDI engine with early injection. The engine operated at $\lambda \sim 1.6$ with acceptable COV_{imep} slightly greater than 5%. Leaning the mixture prolonged the flame evolution process with overall lower flame intensity. The reacting species obtained from flame spectroscopy such as OH, CO_2, O, and soot spectroscopy signals were in lower concentrations for the mixture having a higher air–fuel ratio. Thus, lean mixtures resulted in reduced polluting species and ensured much less particle formation. Also, flame circularity reduced as the equivalence ratio was decreased. Strongly induced fluid flow such as swirl and tumble effectively extends the lean limit or reduces combustion variability. Studies have shown their role in improving engine performance (Zhang et al. 2014; Matsuda et al. 2017). However, these advantages are obtained at the cost of reduced volumetric efficiency in a naturally aspirated engine. Boosting along with organized flow can result in desired engine performance. In a study performed by Yang et al. (2019), different tumble deflectors were incorporated in the intake manifold, which augmented the tumble ratio of fluid motion from 0.5 to 1.5 and 2.2 in spray-guided DISI engines. The study reported an increase in flame development rate by 13.9% and 34.5%, increasing the tumble ratio of 1.5 and 2.2. The TKE of in-cylinder flow increased with a higher tumble, enhancing the fuel–air mixing and intensifying mass transfer between the burnt and unburnt zones. A more blueish flame was observed for a higher tumble. The propensity of yellow flames reduced and delayed, as shown in Fig. 7.24. Calculation of presence probability images of flames showed that for a tumble ratio of 0.5, the flame development was slower with higher cyclic variations. Repeatability and faster flame propagation were observed for a tumble ratio of 2.2. Hence, optimizing the tumble ratio for improved engine performance and reduced cyclic variations can be effective for GDI engines, especially for leaner mixture combustion.

The highly organized flows were also investigated to reduce the variability in the in-cylinder conditions and provide good combustion stability. For stratified operation in a spray-guided engine, fuel injection and ignition are closely coupled. Therefore, the high flow velocities and turbulence could affect the flames. Further, the presence of steep gradients in the fuel concentration and flow velocities may induce unfavourable conditions for early flame growth. In a study by Zeng et al. (2016), the deterioration of the combustion performance of stratified mixture caused by increased

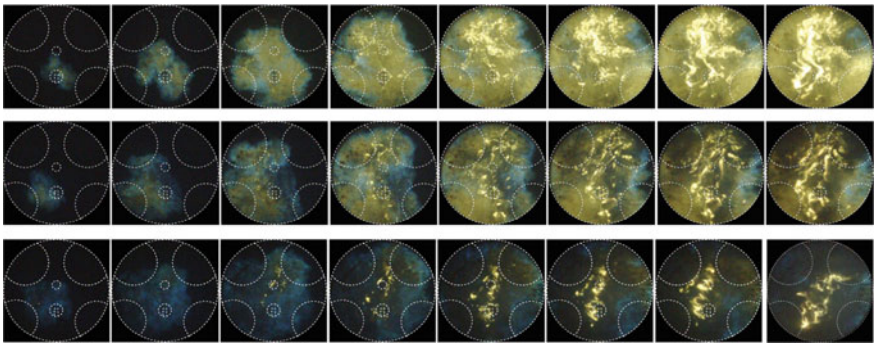

Fig. 7.24 Combustion images for different tumble ratios (Yang et al. 2019)

speed was prevented by swirl enhanced intake airflow. The authors mentioned that the poor burning cycles were dependent on variability in the early flame growth. The regression of burning rate in the later combustion period was also a factor affecting the combustion cycles. The spray-flow interaction analysis revealed that spray from a multi-hole injector redistributed the swirl-enhanced flow momentum and better-centred vortex formation with reduced variability. The flame imaging results showed that the kernel randomly stretched without swirl based on the ignition of two spray plumes stranding on either side of the spark plug. While, in case of enhanced swirl, flame kernel repeatedly convected towards the specific spray plume, resulting in repeatable ignition. Hung et al. (2014) conducted a study to examine the effect of swirl (swirl ratio of 0.55 and 5.68) on the early flame development in the spray-guided DISI engine. Highly directed swirl flow (5.68) advanced the initial frame kernel origin by 4° CA compared to low swirl. Flame kernel propagation speed during early flame growth was enhanced by two times w.r.t. the low swirl case. Hence, peak pressure location also advanced, which improved the engine power output. The location of flame centroid was also highly repeatable for the higher swirl case, which resulted in lower cyclic variations in the combustion characteristics.

Though direct injection of fuel offers the advantage of in-cylinder charge cooling, which helps reduce knock compared to port-injected engines, the complexity involved in proper fuel–air mixture distribution, charge inhomogeneity, fuel impingement and boosting leads to favourable conditions for engine knock. With the help of optical diagnostics, the in-situ processes responsible for knocking and its relationship with engine variables can be understood. In a study by Catapano et al. (2017), UV–visible flame imaging was done for a high spatial and temporal description of knocking characteristics in a multi-cylinder turbocharged wall-guided GDI engine. It was observed that split-injection strategies were effective in suppressing the knocking. Flame visualization allowed tracking of the normal flame propagation, end-gas auto ignition, and residual flames under knock, which correlated well with the knocking parameters obtained via in-cylinder pressure measurements. Close correlations were found between the pressure oscillations due to knock onset

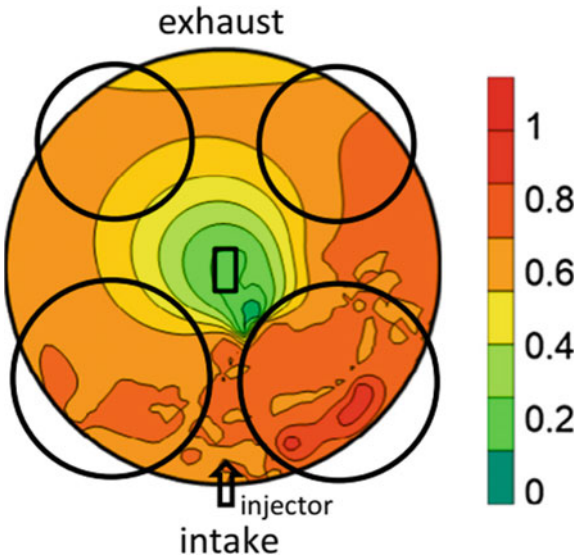

Fig. 7.25 Probability maps for secondary flames (Merola et al. 2016a)

and negative flame front curvature. The authors worked on a novel way of determining knock onset's temporal and spatial location by analyzing centroid luminosity dynamics. Merola et al. (2016a) investigated the hot-spot induced pre-ignition and secondary flame analysis leading to abnormal combustion in wall-guided GDI engines. Knocking cycles were observed with the secondary flames near the cylinder walls. The knock intensity was found to be correlated with the area of secondary flames. In Fig. 7.25, it can be seen that the higher probability regions of secondary flames near the cylinder wall were towards the injector location. It inferred that the fuel deposits were mainly responsible for abnormal combustion, as the engine was devoid of oil droplets. Further, the initiation of abnormal combustion from hot-spot induced pre-ignition was less evident.

The engine researchers further need to consider the diversification of fuels since bio-components can reduce global CO_2 emissions. However, the biofuels differ in chemical and physical properties, affecting the mixture formation and combustion characteristics. Hence, it is essential to understand the in-cylinder combustion phenomena for different biofuels to manage fuel flexibility and fuel utilization better. Catapano et al. (2013) optically investigated the combustion process of ethanol and gasoline fuelling in a small DISI engine having a side-mounted injector. Chemiluminescence imaging was done via ICCD camera for flame visualization, and soot formation analysis was done using a CCD colour camera by 2-colour pyrometry. The intensity of diffusive flames lowered for higher FIP due to improved mixture homogeneity. Ethanol combustion resulted in considerably lower diffusive flames. The KL factor obtained for soot analysis was lower for ethanol combustion owing to its

chemical properties. In another study (Catapano et al. 2016), authors attempted endoscopic imaging of a multi-cylinder turbocharged engine. E50 and E85 showed higher integral flame luminosity during the early combustion phase due to enhanced flame speed. However, gasoline and E10 exhibited higher diffusive flames in the later phase, when the flame front devoured the piston fuel film. These observations correlated well with lower UHC and smoke emissions for E50 and E85. Quicker fuel vaporisation and higher oxygen content in ethanol-blended gasoline improved homogenization, increased flame speed, and reduced soot emissions. In a study by Sementa et al. (2012), it was found that in ethanol combustion, diffusive flames were less visible, which was also evident from low soot obtained from the 2-colour pyrometry. Apart from methanol and ethanol, butanol was also investigated as a fuel of interest due to recent developments in its bio-based production pathways. Its fuel properties are comparable to gasoline, such as calorific value and corrosiveness. However, butanol has four isomers, and their molecular structure could affect combustion. In a study by Han et al. (2020), different butanol isomers, namely n-butanol, sec-butanol, iso-butanol and tert-butanol, were blended with gasoline surrogates, PRF/TPRF in a 3:7 ratio and investigated for flame characteristics. Butanol addition resulted in slower flame development as compared to gasoline surrogates due to longer ignition delay. Higher viscosity and surface tension of butanol resulted in larger spray droplets which slowed down the fuel–air mixing. Higher LHV also led to reduced mixture reactivity. Among all isomers, n-butanol showed the fastest flame propagation due to a straight-chain structure, while tert-butanol exhibited the slowest flame. However, their PN emission reduction capability ranked in order of sec- > iso- > n- > tert-. Merola et al. (2016b) performed spatially resolved UV–visible flame visualization for butanol as a complete gasoline replacement in a wall-guided optically accessible GDI engine. Both fuels showed macro-distortion in flames during throttled operation. However, at WOT, butanol flames showed higher Heywood Factor values at both stoichiometric and lean operation. Gasoline flames were more luminous, with continuous strong emission between 300 and 550 nm wavelength, including OH and CH bands. Higher fluctuation in intensity luminous integral signals for gasoline flames indicated higher cyclic variations. Koupaie et al. (2019) reported that faster combustion was observed with alcohol addition. Flames tend to propagate towards the exhaust valve side. Placing the spark plug slightly biased towards the intake valve side could resolve the issue of exhaust migration characteristics and symmetric flame development. However, the maximization of inlet valve size could be a possible constraint in this.

Natural gas-fuelled engines also get attention due to lower carbonaceous emissions despite reduced engine power output and thermal efficiency. Though, late direct injection of natural gas offers favourable conditions for improved engine performance. In one such study by Chen et al. (2019), methane combustion in leaner conditions was investigated for varying injection timings. The latest injection timing (~100° CA) reported the highest flame propagation speed (increment of 50%). Late injection promoted in-cylinder turbulence and volumetric efficiency (due to injection at IVC), resulting in faster combustion. Di Iorio et al. (2016) investigated the effect of hydrogen enrichment of methane on combustion characteristics. Hydrogen

addition enhanced the flame speed due to the higher diffusivity of hydrogen. The improved mixing enhanced the homogeneity, leading to uniform flame propagation. Hence, lower carbonaceous emissions were reported for hydrogen-methane blends. Di Iorio et al. (2016) performed flame analysis for different fuels, namely methane, ethanol, butanol, isooctane and gasoline, in a spray-guided optical DISI engine. Engine encompasses a multi-hole injector with a FIP of 150 bar. Experiments were done at a fixed engine speed of 1500 RPM and 0.5 bar intake pressure. For methane, the injection was done in the intake plenum to achieve a homogeneous mixture, which was considered the baseline for other fuels injected earlier into the cylinder. Effect of equivalence ratio ($\varphi = 1$ and 0.83) and coolant temperature (20 and 90 °C) were also investigated for flame characteristics. The study reported that post ignition at $\varphi = 1$, flame growth was the fastest for ethanol, followed by butanol, gasoline and isooctane. Methane reported slower flame growth during the initial flame development stage. However, after 20–25° aSOI, its flame grew at a speed of 10–13 m/s, similar to alcohols. Trends of flame speed were similar at both coolant temperatures, where 90 °C showed 5–10% higher values. Calculations of turbulent flame speeds revealed that the burning velocity of butanol was ~8% lower than ethanol but ~5% faster than gasoline. The flame centroid path for all test fuels was similar towards the exhaust valves. Global flame centroid displacement speed was common and fairly stable for all test fuels of the order of 2 m/s. However, there were differences in flame texture among different test fuels. Alcohols and methane flames showed comparatively lower luminosities than isooctane and gasoline. In another study (Aleiferis and Behringer 2015), authors attempted chemiluminescence imaging and double-pulsed laser-illuminated flame tomography to characterize flame characteristics and quantify the flame front topology, respectively. Variations in flame speed for different test fuels were similar to the previous study. However, flame speed obtained from the flame tomography was independent of equivalent flame radii, while from the chemiluminescence imaging, flame speeds were higher for the higher flame radii. Flame roundness was of the order of ~10–15%, with ethanol having the highest, followed by butanol, gasoline and iso-octane. This showed that flames from hydrocarbon fuels exhibited a higher level of distortion and multiple cluster levels than alcohols.

Despite GDI engine technology offering many advantages in terms of engine performance, it results in high particulate emissions. The formation of ultrafine or fine particles in the exhaust becomes unavoidable due to the availability of locally rich zones due to incomplete fuel–air mixing, stratified mixture, and fuel film formation on the combustion chamber walls. Researchers focus on reducing particulate emissions from the engine as it poses a serious risk to the environment and human health. Hence, it is important to understand the soot formation mechanism in greater detail. Several researchers have studied the in-cylinder soot formation process via optical diagnostics techniques such as the 2-colour pyrometry (2C), LII and Laser Extinction Method (LEM) (Pastor et al. 2016; Wang et al. 2018). In one such study by Xie et al. (2021), 2-colour LII was applied to evaluate soot volume fraction, soot evolution, and distribution in a single-cylinder optical GDI engine having a side-mounted injector. It was found that with an increase in the fuel injection quantity, soot volume fraction in a measured plane increased and then decreased. It also led to increased non-uniformity

of soot distribution. The soot formed peaked at around 42° CA aTDC, and afterwards, it decreased due to the oxidation. A dominant factor behind soot formation was the pool fire which was evident till 52° CA aTDC. Later, the produced soot gathered around a 10 mm plane. The produced soot reached a balanced state after 82° CA aTDC and was distributed throughout the combustion chamber following the in-cylinder flows. In a study by de Francqueville et al. (2010), soot volume fraction was obtained using a coupled application of LII and LEM in a stratified spray-guided combustion system. The soot levels were measured in a vertical plane for different injection strategies and EGR. Double injections decreased the soot while EGR promoted the soot formation. The results supported a commonly understood hypothesis. Rapid formation of soot took place with combustion. The fuel-rich zones were mainly responsible for soot production. Soot oxidation and soot formation were competing phenomenon occurring during the expansion stroke. There was a sharp reduction in soot due to oxidants such as OH radicals. The oxidation process was detected significantly till 90° aTDC, after which the in-cylinder temperature became too low to sustain these reactions. Hence, air–fuel mixing, local fuel-rich zones and oxidant concentrations are the key factors determining the soot formation. Potenza et al. (2020) demonstrated a neural network two colours (NNTC) method for quantifying the soot concentration in a GDI engine. The values obtained from NNTC were in good agreement with exhaust soot measurement. Apart from this, several studies used the KL factor and 2-colour method to determine the soot concentration. The study found that SOI variations had a profound effect on the soot concentration compared to rail pressure variations.

Hence, from the above discussion, it can be summarised that optical diagnostics techniques have immensely contributed to understanding different complex in-cylinder phenomenon and their interactions in very short time scales in the DISI engines. Although implementing these tools helps obtain optimized engine design features and control parameters in a wide range of engine operating conditions, several scarcely understood or completely unknown aspects of the in-cylinder processes remained. Further development of these diagnostic tools will enable the scientific community to utilize their potential in developing advanced GDI engines beyond the current limitations.

7.3 Summary and Way-Forward

Optical diagnostics is a well-established research tool for advanced combustion development. Future advancements require developing more sophisticated high-speed imaging capabilities to study coupled, non-linear processes and generate accurate data for critical model validation. Demand for multiple signal acquisitions and their synchronization with optical instruments is bound to increase in future. Simultaneous deployment of multiple optical tools is of great interest for researchers to understand the coupled and complex relationships in engine processes. Greater focus is required on generating time-resolved three-dimensional engine data. Data

acquisition and processing systems would have to be more powerful to handle an enormous amount of data acquired during experimental measurements. Multiphase flow measurement capabilities need to be further improved to characterize spray-flow interactions and processes involved in the formation and destruction of soot. In-situ measuring equipment working in high pressure and temperature conditions need to be improved. More work is required for higher resolution measurements for studying the liquid–gas interactions and related surface properties measurements. More work should focus more on developing endoscopic tools than research studies, which would boost their availability and capability. Optical diagnostics has been a crucial component in developing superior engines and would continue to play an increasingly more important role. A growing interest in direct injection technologies has resulted in an increased number of in-cylinder investigations. Phenomenons such as multiphase flow, spray-wall impingement, spray-flow interactions, charge stratification, partially premixed combustion and soot formation that were not of much importance in port-injected SI engines have become very important in GDI engines. The application of optical diagnostic tools to investigate the effect of engine control parameters on the in-cylinder flows, mixture formation, and subsequent combustion processes would help optimise the engine for obtaining superior performance and reducing emissions.

References

Aleiferis PG, Behringer MK (2015) Flame front analysis of ethanol, butanol, iso-octane and gasoline in a spark-ignition engine using laser tomography and integral length scale measurements. Combust Flame 162(12):4533–4552

Attar MA, Herfatmanesh MR, Zhao H, Cairns A (2014) Experimental investigation of direct injection charge cooling in optical GDI engine using tracer-based PLIF technique. Exp Thermal Fluid Sci 59:96–108

Badawy T, Attar MA, Xu H, Ghafourian A (2018) Assessment of gasoline direct injector fouling effects on fuel injection, engine performance and emissions. Appl Energy 220:351–374

Bao Y, Chan QN, Kook S, Hawkes E (2014) A comparative analysis on the spray penetration of ethanol, gasoline and iso-octane fuel in a spark-ignition direct-injection engine (No. 2014-01-1413). SAE technical paper

Bardi M, Di Lella A, Bruneaux G (2019) A novel approach for quantitative measurements of preferential evaporation of fuel by means of two-tracer laser-induced fluorescence. Fuel 239:521–533

Catapano F, Sementa P, Vaglieco BM (2013) Optical characterization of bio-ethanol injection and combustion in a small DISI engine for two wheels vehicles. Fuel 106:651–666

Catapano F, Sementa P, Vaglieco BM (2016) Air-fuel mixing and combustion behaviour of gasoline-ethanol blends in a GDI wall-guided turbocharged multi-cylinder optical engine. Renew Energy 96:319–332

Catapano F, Sementa P, Vaglieco BM (2017) Characterization of knock tendency and onset in a GDI engine by means of conventional measurements and a non-conventional flame dynamics optical analysis. SAE Int J Engines 10(5):2439–2450

Chan QN, Bao Y, Kook S (2014) Effects of injection pressure on the structural transformation of flash-boiling sprays of gasoline and ethanol in a spark-ignition direct-injection (SIDI) engine. Fuel 130:228–240

Chen H, Lillo PM, Sick V (2016) Three-dimensional spray–flow interaction in a spark-ignition direct-injection engine. Int J Engine Res 17(1):129–138
Chen L, Wei H, Zhang R, Pan J, Zhou L, Liu C (2019) Effects of late injection on lean combustion characteristics of methane in a high compression ratio optical engine. Fuel 255:115718
Clark LG, Kook S (2018) Correlation of spatial and temporal filtering methods for turbulence quantification in spark-ignition direct-injection (SIDI) engine flows. Flow Turbul Combust 101(1):161–189
Clark LG, Kook S, Chan QN, Hawkes E (2018) The effect of fuel injection timing on in-cylinder flow and combustion performance in a spark-ignition direct-injection (SIDI) engine using particle image velocimetry (PIV). Flow Turbul Combust 101(1):191–218
Clark LG, Kook S, Chan QN, Hawkes ER (2014) Effects of injection timing and spark timing on flame propagation in an optically accessible spark-ignition direct-injection (SIDI) engine. In: 19th Australasian fluid mechanics conference, pp 350–356
Clark LG, Kook S, Chan QN, Hawkes ER (2016) Multiple injection strategy investigation for well-mixed operation in an optical wall-guided spark-ignition direct-injection (WG-SIDI) engine through flame shape analysis (No. 2016-01-2162). SAE technical paper
Clark LG, Kook S, Chan QN, Hawkes ER (2017) Influence of injection timing for split-injection strategies on well-mixed high-load combustion performance in an optically accessible Spark-Ignition Direct-Injection (SIDI) engine (No. 2017-01-0657). SAE technical paper
de Francqueville L, Bruneaux G, Thirouard B (2010) Soot volume fraction measurements in a gasoline direct injection engine by combined laser-induced incandescence and laser extinction method. SAE Int J Engines 3(1):163–182
Deschamps B, Ricordeau V, Depussay E, Mounaïm-Rousselle C (1999) Combined catalytic hot wires probe and fuel-air-ratio-laser induced-exciplex fluorescence air/fuel ratio measurements at the spark location prior to ignition in a stratified GDI engine. SAE Trans 1631–1641
Di Iorio S, Sementa P, Vaglieco BM (2016) Analysis of combustion of methane and hydrogen–methane blends in small DI SI (direct injection spark ignition) engine using advanced diagnostics. Energy 108:99–107
Drake MC, Fansler TD, Lippert AM (2005) Stratified-charge combustion: modelling and imaging of a spray-guided direct-injection spark-ignition engine. Proc Combust Inst 30(2):2683–2691
Fraidl GK, Piock WF, Wirth M (1996) Gasoline direct injection: actual trends and future strategies for injection and combustion systems. SAE Trans 543–559
Geschwindner C, Kranz P, Welch C, Schmidt M, Böhm B, Kaiser SA, De la Morena J (2020) Analysis of the interaction of spray G and in-cylinder flow in two optical engines for late gasoline direct injection. Int J Engine Res 21(1):169–184
Han D, Fan Y, Sun Z, Nour M, Li X (2020) Combustion and emissions of isomeric butanol/gasoline surrogates blends on an optical GDI engine. Fuel 272:117690
Hung DL, Chen H, Xu M, Yang J, Zhuang H (2014) Experimental investigation of the variations of early flame development in a spark-ignition direct-injection optical engine. J Eng Gas Turbines Power 136(10)
Ipp W, Egermann J, Engermannn J, Wagner V, Leipertz A (2000) Visualization of the qualitative fuel distribution and mixture formation inside a transparent GDI engine with 2D MIE and LIEF techniques and comparison to quantitative measurements of the air/fuel ratio with 1D Raman spectroscopy. SAE Trans 931–941
Irimescu A, Merola SS, Martinez S (2018) Influence of engine speed and injection phasing on lean combustion for different dilution rates in an optically accessible wall-guided spark ignition engine. SAE Int J Engines 11(6):1343–1370
Kalwar A, Agarwal AK (2020) Overview, advancements and challenges in gasoline direct injection engine technology. In: Advanced combustion techniques and engine technologies for the automotive sector. Springer, Singapore, pp 111–147
Kalwar A, Agarwal AK (2021) Lean-burn combustion in direct-injection spark-ignition engines. In: Alternative fuels and advanced combustion techniques as sustainable solutions for internal combustion engines. Springer, Singapore, pp 281–317

Kang JJ, Kim DJ (2003) Effects of piston shapes and intake flow on the behaviour of fuel mixtures in a GDI engine. KSME Int J 17(12):2027–2033
Koupaie MM, Cairns A, Xia J, Vafamehr H, Lanzanova T (2019) Cyclically resolved flame and flow imaging in an alcohol-fuelled SI engine. Fuel 237:874–887
Lee Z, Kim D, Park S (2020) Effects of spray behaviour and wall impingement on particulate matter emissions in a direct injection spark ignition engine equipped with a high-pressure injection system. Energy Convers Manag 213:112865
Marseglia G, Costa M, Catapano F, Sementa P, Vaglieco BM (2017) Study about the link between injection strategy and knock onset in an optically accessible multi-cylinder GDI engine. Energy Convers Manage 134:1–19
Martinez S, Irimescu A, Merola SS, Lacava P, Curto-Riso P (2017) Flame front propagation in an optical GDI engine under stoichiometric and lean-burn conditions. Energies 10(9):1337
Martinez S, Merola S, Irimescu A (2019) Flame front and burned gas characteristics for different split injection ratios and phasing in an optical GDI engine. Appl Sci 9(3):449
Matsuda M, Yokomori T, Iida N (2017) Investigation of cycle-to-cycle variation of turbulent flow in a high-tumble SI engine (No. 2017-01-2210). SAE technical paper
Merola SS, Tornatore C, Irimescu A (2016a) Cycle-resolved visualization of pre-ignition and abnormal combustion phenomena in a GDI engine. Energy Convers Manag 127:380–391
Merola SS, Tornatore C, Irimescu A, Marchitto L, Valentino G (2016b) Optical diagnostics of early flame development in a DISI (direct injection spark ignition) engine fueled with n-butanol and gasoline. Energy 108:50–62
Naber JD, Siebers DL (1996) Effects of gas density and vaporization on penetration and dispersion of diesel sprays. SAE Trans 82–111
Oh H, Bae C (2013) Effects of the injection timing on spray and combustion characteristics in a spray-guided DISI engine under lean-stratified operation. Fuel 107:225–235
Pastor JV, Garcia-Oliver JM, Garcia A, Mico C, Möller S (2016) Application of optical diagnostics to the quantification of soot in n-alkane flames under diesel conditions. Combust Flame 164:212–223
Peterson B, Reuss DL, Sick V (2011) High-speed imaging analysis of misfires in a spray-guided direct injection engine. Proc Combust Inst 33(2):3089–3096
Peterson B, Reuss DL, Sick V (2014) On the ignition and flame development in a spray-guided direct-injection spark-ignition engine. Combust Flame 161(1):240–255
Pilla G, Kumar R, Laget O, De Francqueville L, Dauphin R, Solari JP (2016) Simulation and optical diagnostics to characterize low octane number dual fuel strategies: a step towards the octane on-demand engine. SAE Int J Fuels Lubr 9(3):443–459
Potenza M, Milanese M, Naccarato F, de Risi A (2020) In-cylinder soot concentration measurement by Neural Network Two Colour technique (NNTC) on a GDI engine. Combust Flame 217:331–345
Sementa P, Vaglieco BM, Catapano F (2012) Thermodynamic and optical characterizations of a high-performance GDI engine operating in homogeneous and stratified charge mixture conditions fueled with gasoline and bio-ethanol. Fuel 96:204–219
Sharma N, Bachalo WD, Agarwal AK (2020) Spray droplet size distribution and droplet velocity measurements in a firing optical engine. Phys Fluids 32(2):023304
Sick V (2010) Optical diagnostics for direct injection gasoline engine research and development. In: Advanced direct injection combustion engine technologies and development. Woodhead Publishing, UK, pp 260–286
Song J, Kim T, Jang J, Park S (2015) Effects of the injection strategy on the mixture formation and combustion characteristics in a DISI (direct injection spark ignition) optical engine. Energy 93:1758–1768
Song J, Lee Z, Song J, Park S (2018) Effects of injection strategy and coolant temperature on hydrocarbon and particulate emissions from a gasoline direct injection engine with high-pressure injection up to 50 MPa. Energy 164:512–522
Song J, Park S (2015) Effect of injection strategy on the spray development process in a single-cylinder optical GDI engine. Atomization Sprays 25(9)

Steeper RR, Stevens EJ (2000) Characterization of combustion, piston temperatures, fuel sprays, and fuel-air mixing in a DISI optical engine (No. 2000-01-2900). SAE technical paper

Stiehl R, Bode J, Schorr J, Krüger C, Dreizler A, Böhm B (2016) Influence of intake geometry variations on in-cylinder flow and flow–spray interactions in a stratified direct-injection spark-ignition engine captured by time-resolved particle image velocimetry. Int J Engine Res 17(9):983–997

Stiehl R, Schorr J, Krüger C, Dreizler A, Böhm B (2013) In-cylinder flow and fuel spray interactions in a stratified spray-guided gasoline engine investigated by high-speed laser imaging techniques. Flow Turbul Combust 91(3):431–450

Wang Y, Makwana A, Iyer S, Linevsky M, Santoro RJ, Litzinger TA, O'Connor J (2018) Effect of fuel composition on soot and aromatic species distributions in laminar, co-flow flames. Part 1. Non-premixed fuel. Combust Flame 189:443–455

Williams B, Edwards M, Stone R, Williams J, Ewart P (2014) High precision in-cylinder gas thermometry using laser-induced gratings: quantitative measurement of evaporative cooling with gasoline/alcohol blends in a GDI optical engine. Combust Flame 161(1):270–279

Xie F, Zhang M, Wang Y, Su Y, Hong W, Cheng P (2021) Soot development in an optical direct injection spark ignition engine fueled with isooctane. Int J Automot Technol 22(2):455–463

Yang J, Dong X, Wu Q, Xu M (2019) Effects of enhanced tumble ratios on the in-cylinder performance of a gasoline direct injection optical engine. Appl Energy 236:137–146

Zeng W, Sjöberg M, Reuss DL (2015) PIV examination of spray-enhanced swirl flow for combustion stabilization in a spray-guided stratified-charge direct-injection spark-ignition engine. Int J Engine Res 16(3):306–322

Zeng W, Sjöberg M, Reuss DL, Hu Z (2016) The role of spray-enhanced swirl flow for combustion stabilization in a stratified-charge DISI engine. Combust Flame 168:166–185

Zeng W, Sjöberg M, Reuss DL, Hu Z (2017) High-speed PIV, spray, combustion luminosity, and infrared fuel-vapour imaging for probing tumble-flow-induced asymmetry of gasoline distribution in a spray-guided stratified-charge DISI engine. Proc Combust Inst 36(3):3459–3466

Zhang Z, Zhang H, Wang T, Jia M (2014) Effects of tumble combined with EGR (exhaust gas recirculation) on the combustion and emissions in a spark-ignition engine at part loads. Energy 65:18–24